

SX Phoenicis Stars in the Globular Cluster NGC 5466

Young-Beom Jeon

Korea Astronomy Observatory, Daejeon 305-348, KOREA

Email: ybjeon@boao.re.kr

Myung Gyoon Lee ¹

Astronomy Program, School of Earth and Environmental Sciences, Seoul National

University, Seoul 151-742, KOREA

Email: mglee@astrog.snu.ac.kr

Seung-Lee Kim

Korea Astronomy Observatory, Daejeon 305-348, KOREA

Email: slkim@kao.re.kr

and

Ho Lee

Department of Earth Science Education, Korea National University of Education,

Choongbuk 363-791, KOREA

Email: leeho119@boao.re.kr

Received _____; accepted _____

¹Visiting Investigator at the Department of Terrestrial Magnetism, Carnegie Institution of Washington, 5241 Broad Branch Road, N.W., Washington, D. C., USA

ABSTRACT

Through time-series CCD photometry of the globular cluster NGC 5466, we have detected nine SX Phoenicis stars including three new ones. All the SX Phoenicis stars are located in the blue straggler region in the color-magnitude diagram of NGC 5466. Five of them show clearly double-radial mode features, the periods of which are well consistent with the theoretical ratio of the first overtone mode to the fundamental mode (P_{1H}/P_F). Normally, it has not been easy to secure a P-L relation of the SX Phoenicis stars, because determination of the pulsational mode of the SX Phoenicis stars has been difficult. The existence of five SX Phoenicis stars in NGC5466 with double-radial modes allows us to derive reliably a P-L relation for the fundamental mode of the SX Phoenicis stars. Using seven SX Phoenicis stars including five stars with double-radial modes, we derive a P-L relation for the fundamental mode in NGC 5466, $\langle V \rangle = -3.25(\pm 0.46)\text{Log}P + 14.70(\pm 0.06)$, ($\sigma = \pm 0.04$), corresponding to $\langle M_V \rangle = -3.25(\pm 0.46)\text{Log}P - 1.30(\pm 0.06)$ for an adopted distance modulus of $(m - M)_0 = 16.00$ and zero reddening.

Subject headings: Globular clusters: individual (NGC 5466) — stars: blue straggler stars — stars: oscillations — stars: variable stars

1. Introduction

NGC 5466 (R.A. = $14^h 05^m 27.3$, Decl. = $+28^\circ 32' 04''$, J2000.0) is a sparse globular cluster with an extremely low metallicity $[\text{Fe}/\text{H}] = -2.22$ (Harris 1996), having a large number of blue stragglers. Nemec & Harris (1987) found 48 blue straggler stars (BSSs) which are mostly concentrated within $r = 3'$ from the center of the cluster. Several kinds of variables stars are known to exist in this cluster: six SX Phoenicis stars (Nemec & Mateo 1990; Chen & Corwin 1999), three eclipsing binaries (Mateo et al. 1990; Kallrath, Milone & Stagg 1992; McKinley & Corwin 1998), a Cepheid and more than twenty RR Lyrae stars (Clement 2001).

In this paper we present a photometric study of SX Phoenicis stars in NGC 5466. In the long-term search for the short-period variable stars in Galactic globular clusters, we have found three new SX Phoenicis stars named Cl* NGC 5466 SXP 1, Cl* NGC 5466 SXP 2 and Cl* NGC 5466 SXP 3 in addition to the previously known six named Cl* NGC 5466 NH 27, Cl* NGC 5466 NH 29 Cl* NGC 5466 NH 35, Cl* NGC 5466 NH 38, Cl* NGC 5466 NH 39 and Cl* NGC 5466 NH 49 by Nemec & Mateo (1990); hereafter referred to as SXP1, SXP2 and SXP3 for new ones, and NH27, NH29, NH35, NH38, NH39 and NH49 for known ones, respectively. Results on the eclipsing binaries, a Cepheid and RR Lyrae stars in NGC5466 will be presented in a separate paper (Lee et al. 2004). We adopt the zero interstellar reddening and the distance modulus $(m - M)_0 = 16.00$ in this study (Harris 1996).

This paper is composed as follows. Observations and data reduction are described in § 2. § 3 describes selection of variable stars in NGC 5466, and § 4 presents the light curves and frequency analysis of the SX Phoenicis stars. § 5 discusses the characteristics of these SX Phoenicis stars, including mode identification and the P-L relation. Finally primary results are summarized in § 6.

2. Observations and Data Reduction

2.1. Observations

We obtained time series CCD images of NGC 5466 for 22 nights from February 8th, 1999 to March 23rd, 2002. Total observing time is 27.1 and 133.7 hours for B and V bands, respectively. A total of 48 and 944 frames were obtained for B and V bands, respectively. Because the observations were performed under various seeing (0.9~4.5 arcsec) and weather conditions, we adjusted exposure times depending on the seeing and transmission of the night sky. The observation log is listed in Table 1.

EDITOR: PLACE TABLE 1 HERE.

The CCD images were obtained with a thinned SITe 2k CCD camera attached to the 1.8m telescope at the Bohyunsan Optical Astronomy Observatory (BOAO) in Korea. The field of view of a CCD image is $11'.6 \times 11'.6$ ($0.3438 \text{ arcsec pixel}^{-1}$) at the f/8 Cassegrain focus of the telescope. The readout noise, gain and readout time of the CCD are 7.0 e^- , $1.8 \text{ e}^-/\text{ADU}$ and 100 seconds, respectively.

A greyscale map of a V band CCD image is shown in Figure 1. It shows only a central region ($7'.6 \times 5'.7$) of the cluster, out of the total observing field of $11'.6 \times 11'.6$. Nine SX Phoenicis stars are represented by circles labeled their names in Figure 1.

EDITOR: PLACE FIGURE 1 HERE.

2.2. Data Reduction

Using the IRAF/CCDRED package, we processed the CCD images to correct overscan regions, trim unreliable subsections, subtract bias frames and flatten images. Instrumental

magnitudes were obtained using the point spread function (PSF) fitting photometry routine in the IRAF/DAOPHOT package (Stetson 1987; Massey & Davis 1992). Nemec & Harris (1987) presented photoelectric photometry of 36 stars in the outer region of NGC 5466, of which we select ten stars for the standardization of the instrumental magnitudes. They are located in our observing fields. For standardization, we selected nine and five frames for V and B bands, respectively, taken under good seeing conditions on March 12, 2002. The derived transformation equations are

$$V = v + \text{constant} - 0.071(\pm 0.01)(B - V), \quad (1)$$

$$B = b + \text{constant} + 0.169(\pm 0.01)(B - V), \quad (2)$$

where v and b are instrumental magnitudes of V and B bands, respectively. The color coefficients are average values for nine frames for V band and five frames for B band, respectively. *Constants* are the zero points of the individual frames. Finally, we have obtained the standard magnitudes of the stars by averaging the magnitudes of all the frames. The residuals between photoelectric magnitudes and derived magnitudes for standard stars are $\Delta V = -0.001 \pm 0.027$ and $\Delta(B - V) = 0.005 \pm 0.056$, respectively. There are no systematic deviations depending on magnitudes or colors.

3. Selection of Variable Stars

In Figure 2 we display $(V, B - V)$ diagram of a total of about 10,600 stars in the observing field of NGC 5466. The left panel shows the color-magnitude diagram (CMD) for a central region at $r < 1.0$, and the right panel shows the CMD for an outer region at $r \geq 1.0$.

EDITOR: PLACE FIGURE 2 HERE.

In Figure 2 the main sequence (MS), the red giant branch (RGB) and the horizontal branch (HB) are clearly seen on both panels. In addition, there are about 60 stars at the brighter and bluer region above the MS turnoff (represented by boxes on both panels), which are blue stragglers.

We applied the ensemble normalization technique (Gilliland & Brown 1988; Jeon et al. 2001) to normalize instrumental magnitudes between time-series CCD frames. We used about a hundred normalizing stars ranging from 13.7 mag to 19.0 mag for the V band and from 13.7 mag to 18.5 mag for the B band. We exclude variable stars and stars located within $r = 0.5$ to avoid the crowding effects. For B band data, we use them only for obtaining mean magnitudes, because the data quality was not good enough to apply frequency analysis. The normalization equation we used is

$$B \text{ or } V = m + c_1 + c_2(B - V) + c_3P_x + c_4P_y \quad (3)$$

where B , V , and m are the standard and instrumental magnitudes of the normalizing stars, respectively. c_1 is the zero point and c_2 is the color coefficient. c_3 and c_4 are used to correct position-dependent terms such as atmospheric differential extinction, flat field error and variable PSF. The typical values of the coefficients are $c_1 = -3.265$, $c_2 = -0.037$, $c_3 = 0.000021$ and $c_4 = -0.000029$. P_x and P_y are the positions in the CCD, which are ranged from 1 to 2048.

After photometric reduction of the time-series frames, we inspected by eyes luminosity variations for about 10,600 stars in the entire field to search for variable stars. From this we have detected nine SX Phoenicis stars. Six of them are previously known, and three are newly discovered in this research. We also recovered previously known 19 RR Lyrae stars, three eclipsing binaries and a Cepheid.

Among the nine SX Phoenicis stars, the three newly discovered ones are designated by SXP1, SXP2 and SXP3. SXP1 is located near a bright star, and SXP2 and SXP3 are

located very close to the center of the cluster and have very low amplitudes (see Figure 3). Although seven of the nine SX Phoenicis stars are located in the central region at $r < 1.5$, we could detect them easily due to the sparseness of the cluster. For the globular clusters M53 (Jeon et al. 2003) and M15 (Jeon et al. 2001), we found SX Phoenicis stars only in the outer region at $r > 2.0$; those clusters have very crowded central regions, so it is very difficult to detect SX Phoenicis stars in their central regions.

The coordinates, mean magnitudes and color indices of the nine SX Phoenicis stars are listed in Table 2.

EDITOR: PLACE TABLE 2 HERE.

The right ascension and declination coordinates (J2000.0) of the stars in Table 2 were obtained from the astrometry using the Guide Star Catalogue (Version 1.1).

4. Light Curves and Frequency Analysis

Figure 3 displays V band light curves of the SX Phoenicis stars.

EDITOR: PLACE FIGURE 3 HERE.

In each panel we show a mean photometric error of each observing night by an errorbar in the left-lower corner. Although NGC 5466 has a well resolved structure, all the SX Phoenicis stars except for NH39 suffer still from contamination effects due to neighbor stars. Some photometric data for the four SX Phoenicis stars located near the cluster center were lost by poor seeing and/or bad sky conditions caused by moon lights or thin clouds. The light curves in Figure 3 show typical characteristics of SX Phoenicis stars, i.e., short periods and low amplitudes.

We have performed multiple-frequency analysis to determine pulsating frequencies of the nine SX Phoenicis stars, using the discrete Fourier transform and linear least-square fitting methods (Kim & Lee 1995; Jeon et al. 2001). Figure 4 displays the power spectra of the light curves for the nine SX Phoenicis stars.

EDITOR: PLACE FIGURE 4 HERE.

Each panel shows the prewhitening process to derive each peak in the power spectrum with window spectra represented in the inner panels.

Low frequencies detected in all the SX Phoenicis stars in NGC 5466 except for NH49 and SXP2 have resulted from variable seeing condition and/or drift during long observing runs from 1999 to 2002. Synthetic light curves obtained from these analyses are superimposed on the data in Figure 3, and they fit the data well. Some unrealistic light curves of NH38 around HJD 2452069.0 are resulted from high-order fitting to small number of data.

The results of the multiple-frequency analysis for the nine SX Phoenicis stars are summarized in Table 3.

EDITOR: PLACE TABLE 3 HERE.

The signal-to-noise ratios are defined to be the square root of the ratio of the power for each frequency to the average power after prewhitening all frequencies. We assume a real frequency to have the amplitude signal-to-noise ratio larger than 4.0 as done by Breger et al. (1993).

During the analysis we detected many harmonic frequencies and probable nonradial frequencies in addition to the primary frequencies of each star. Most of the frequencies

have been affected by 1 cycle day⁻¹ alias effect. The primary period modes for these SX Phoenicis stars range from 0.0386 days to 0.0552 days, and the semi-amplitudes of the variability range from 0.023 mag to 0.221 mag.

We divide the sample of SX Phoenicis stars into three groups: 1) Double-radial mode SX Phoenicis stars (SXP2, SXP3, NH35, NH38 and NH39), 2) Single-radial mode SX Phoenicis stars with long-term variations (SXP1 and NH29), and 3) Single-radial mode SX Phoenicis stars without long-term variations (NH27 and NH49). Individual SX Phoenicis stars in each group are described in appendix.

4.1. Double-Radial Mode SX Phoenicis Stars

Double-radial mode stars are very useful to identify the pulsating modes of SX Phoenicis stars. SXP3, NH35 and NH39 show the double-radial mode oscillations. Their period ratios are $P_{1H}/P_F = 0.7979, 0.7825$ and 0.7826 respectively. The first radial modes are f_3, f_5 and f_3 of SXP3, NH35 and NH39, respectively. The double-radial mode features of these three stars are considered to be intrinsic ones. Interestingly, NH39 shows the combination frequencies of the two radial modes; f_4 and f_6 corresponding to $f_3 - f_1$ and $f_3 + f_1$, respectively. For NH35 f_4 is a suspected harmonic frequency of $f_5 - f_1$ affected by 1 cycle day⁻¹ aliases. The period ratios help us to identify their pulsation modes with confidence. The period ratios of SXP3, NH35 and NH39 are close to the theoretical ratios of the fundamental and first overtone mode for SX Phoenicis stars with extremely low metal abundance (Santolamazza et al. 2001). In Figure 5 we compare the period ratios of SXP3, NH35 and NH39 with the theoretical period ratios for various $\text{Log } L/L_\odot$ with $Z=0.0001$ and $M/M_\odot=1.0$ by Santolamazza et al. (2001).

EDITOR: PLACE FIGURE 5 HERE.

Figure 5 shows that the two double-radial mode SX Phoenixis stars, NH35 and NH39, are located on the $\text{Log } L/L_{\odot}=0.8$ line, and that SXP3 is consistent with the $\text{Log } L/L_{\odot}=0.6$ line. Using Table 2 of Santolamazza et al. (2001) we estimate the temperatures of all these three stars to be about 7700K.

SXP2 and NH38 in Table 3 are also suspected double-radial mode pulsators. But we could not obtain precise frequencies for the secondary radial modes because of the poor data quality. Their period ratios P_{1H}/P_F are 0.764 and 0.810, respectively. These values depart from the theoretical ranges for the ratio of P_{1H}/P_F . The frequencies of the suspected to be secondary radial modes are probably real ones, according to the amplitude signal-to-noise ratios (see Table 3) and features of power spectra in Figure 4. If we assume that they are affected by the 1 cycle day⁻¹ aliases, the period ratios of SXP2 and NH38 can be 0.781 and 0.798, respectively, which are well consistent to the theoretical P_{1H}/P_F . We consider SXP2 and NH38 to be candidates of double-radial mode SX Phoenixis stars.

4.2. Single-Radial Mode SX Phoenixis Stars with Long-Term Variations

SXP1 and NH29 show distinct low frequencies, 1.5616 and 0.4268 cycle day⁻¹, and their V amplitudes are 0.076 and 0.158 mag, respectively. The low frequencies are clearly identified in the power spectra of Figure 4 and in light curves of Figure 3. Their amplitude signal-to-noise ratios are 8.7 and 18.2, respectively. We have checked an existence of bad pixels on the CCD images, finding no bad pixels near these stars. We propose cautiously that the low frequencies of SXP1 and NH29 are caused by a nonradial g -mode and a contact binary, respectively. SXP1 is a very interesting pulsator, if their nonradial mode is real. This is the first discovery in globular clusters for a pulsator which possesses p -mode (characterized by an SX Phoenixis star) and g -mode (characterized by a γ Doradus star), simultaneously. As an example for this type of pulsators, Handler et al. (2002) found the

characteristics of δ Scuti and γ Doradus type pulsations for a field binary HD 209295. But Henry, Fekel & Henry (2004) found that a long-term period component of HD 207651, $1.3598 \text{ cycle day}^{-1} = 0.73540 \text{ day}$, was not resulted from γ Doradus type term but the ellipticity effect. From the spectroscopic observations an eclipsing period was twice the period of the long-term period seen in the photometry.

Figure 6 is a phase diagram of the long period of 2.3430 days for NH29. It shows a distinct light variation. If this is a contact eclipsing binary star, the total period will be about two times of the long-term period. Otherwise, it could be a g-mode frequency similar to the long-term variation of SXP1. Unfortunately the data are not good enough for accurate frequency analysis.

EDITOR: PLACE FIGURE 6 HERE.

5. Discussion

5.1. Characteristics of the SX Phoenicis Stars

In Figure 7, we show the position of the nine SX Phoenicis stars in the color-magnitude diagram of NGC 5466, listing their mean magnitudes and color indices in Table 2. Figure 7 shows that all the SX Phoenicis stars are located in the blue straggler region, brighter and bluer than the main sequence turnoff point. It is known that all the known SX Phoenicis stars in globular clusters are BSSs, but there are non-variable stars among the BSSs.

EDITOR: PLACE FIGURE 7 HERE.

In Figure 8 we have compared the V amplitudes and periods of the SX Phoenicis stars in NGC 5466 (filled circles) with those of SX Phoenicis stars in other globular clusters, field

SX Phoenicis stars and δ Scuti stars.

EDITOR: PLACE FIGURE 8 HERE.

It includes the SX Phoenicis stars in M53 (star symbols) and M15 (a cross) discovered by our previous searches for variable blue stragglers in globular clusters (Jeon et al. 2001, 2003). The sources of the data in Figure 8 are Rodríguez et al. (2000) for field SX Phoenicis stars and δ Scuti stars, and Rodríguez & López-González (2000) for SX Phoenicis stars in Galactic globular clusters. Figure 8 shows that the V amplitudes and periods of the SX Phoenicis stars in NGC 5466 are consistent with those for SX Phoenicis stars in other globular clusters; the V amplitudes increases steeply with increasing period, and the V amplitudes of SX Phoenicis stars are larger than those of δ Scuti stars with the same period.

5.2. Radial Mode Identification

A method for mode identification is to use a pulsation constant, Q , denoted as $Q = P\rho^{1/2}$ where P and ρ are the period and mean density of variable stars, respectively. Q values of overtone mode are smaller than that of the fundamental mode (Breger 2000). Q values can be derived using a photometric method such as Strömgren $uvby$ H_β observation (Rodríguez et al. 2003). Another photometric method is to use SX Phoenicis stars with double-radial mode, but the SX Phoenicis stars with double-radial mode are rare. Fortunately, five (including two candidates) of the SX Phoenicis stars in NGC5466 are found to have double-radial modes, so their modes are identified clearly. All the double-radial mode stars (SXP2, SXP3, NH35, NH38 and NH39) show the fundamental and first overtone modes, as described in § 3.1.

The mode of the rest of the SX Phoenicis stars can be identified using the amplitude,

period and luminosity. NH27 is identified as the first overtone mode because of its V amplitude, 0.246 mag, being slightly lower, and especially the position in the period-magnitude diagram as shown in Figure 9. SXP1 has a high amplitude, and is located in the fundamental region in the period-magnitude diagram. So it is a fundamental mode star. In Table 3, NH35, NH38, NH39 and NH49 show harmonic frequencies supporting asymmetric sinusoidal features. Moreover their total light amplitudes have a range of $0.282 \sim 0.730$ mag, which are characteristics of high amplitude δ Scuti (HADS) stars. So, their mode are clearly identified to be fundamental radial oscillations. Their primary and secondary radial periods correspond to the fundamental and first overtone radial modes, respectively. NH29 is the first overtone mode star according to its low amplitude (0.142 mag), well defined sinusoidal feature in the light curve (see Figure 3) and the location in the period-magnitude diagram. Seven of nine SX Phoenicis stars in NGC 5466 show the fundamental mode or double-radial mode with the fundamental and first overtone modes. They are displayed by open and filled circles in the color-magnitude diagram in Figure 7, respectively. Two filled triangles denote the first overtone mode stars. The identified radial modes are listed in the last column of Table 3.

McNamara (2000, 2001) suggested that the light amplitude and the degree of asymmetry of the light curves are useful parameters for identifying the pulsating modes. Generally this method is very useful for systems with a small number of pulsators and/or no double-radial mode stars therein. However, in many cases these criteria do not give a unique solution to identify pulsating modes, especially for SX Phoenicis stars with very low amplitudes and short periods such as SXP2 and SXP3 in NGC5466.

5.3. Period-Luminosity Relation

The P-L relation of SX Phoenicis stars in the globular clusters is very useful to obtain the distance moduli of the clusters and nearby galaxies (McNamara 1995). However, it is not easy to define well the P-L relation from the observations, because there are often a mixture of different pulsation modes (Jeon et al. 2003; McNamara 2001). But we can easily identify the pulsating mode using the double-radial mode stars as described in the previous section.

Figure 9 presents the P-L relation for the SX Phoenicis stars in NGC 5466.

EDITOR: PLACE FIGURE 9 HERE.

It shows that the sample can be separated into two discrete groups; one is identified as a fundamental mode group (filled circles), and the other is a first overtone mode group (filled triangles and open triangles). The solid line represents the fundamental P-L relation, and the line is shifted to the dashed line corresponding to the first overtone mode stars by the ratio $P_{1H}/P_F = 0.783$. The P-L relation for fundamental mode in NGC 5466 is derived to be

$$\langle V \rangle = -3.25(\pm 0.46) \log P + 14.70(\pm 0.06), \quad (\sigma = \pm 0.04), \quad (4)$$

which corresponds to

$$\langle M_V \rangle = -3.25(\pm 0.46) \log P - 1.30(\pm 0.06) \quad (5)$$

for an adopted distance modulus of $(m - M)_V = 16.00$ and $E(B - V) = 0.00$ (Harris 1996),

The empirical P-L relations have been obtained using field HADS stars and/or cluster SX Phoenicis stars identified by their pulsating modes. The slopes derived by field HADS stars and SX Phoenicis stars in ω Cen show on the whole steeper ones up to -4.66

(McNamara 2000), whereas δ Scuti stars, SX Phoenicis stars in other globular clusters and theoretical results show flatter slopes up to -2.88 (Pych et al. 2001).

The slope of -3.25 for NGC 5466 is in a good agreement with the results for M53 (Jeon et al. 2003) and M55 (Pych et al. 2001). Jeon et al. (2003) obtained a slope of -3.01 for the fundamental mode stars in M53 and Pych et al. (2001) derived a slope of -2.88 for the fundamental mode and a slope of -3.1 for the first overtone mode stars in M55. The slope for NGC 5466 derived in this study agrees also well with the theoretical values of -3.04 by Santolamazza et al. (2001) and -3.05 by Templeton, Basu & Demarque (2002).

6. Summary

Through time-series CCD photometry of the globular cluster NGC 5466, we detect three newly discovered and six known SX Phoenicis stars. Owing to the extremely open, well-resolved structure of NGC 5466, we could detect easily many short period variable stars such as SX Phoenicis stars and eclipsing binaries even in the central region. All the SX Phoenicis stars are found to be located in the blue straggler star region of the CMD. Physical parameters of these stars are summarized in Tables 2 and 3. From the Fourier analysis, we find five double-radial mode stars including two candidates. These stars are very useful to determine the radial modes of SX Phoenicis stars in NGC 5466. These stars show period ratios of the two radial modes which are consistent with the theoretical ratio of the first overtone mode to the fundamental mode (P_{1H}/P_F). Using seven SX Phoenicis stars which are considered to be pulsating in the fundamental mode, we derive a P-L relation for the fundamental mode in NGC 5466, $\langle V \rangle = -3.25(\pm 0.46) \text{Log} P + 14.70(\pm 0.06)$, ($\sigma = 0.04$). The slope of -3.25 for NGC 5466 is in a good agreement with the empirical results for M53 (-3.01 ; Jeon et al. (2003)) and M55 (-2.88 ; Pych et al. (2001)), and the theoretical results of -3.04 by Santolamazza et al. (2001) and -3.05 by Templeton, Basu & Demarque

(2002).

M.G.L. was supported in part by the Korean Research Foundation Grant (KRF-2000-DP0450).

SXP1: It is located very close to a bright star. We could detect four frequencies including a low frequency $f_2 = 1.5616 \text{ cycle day}^{-1}$. f_3 is clearly a harmonic frequency of f_1 corresponding to $2f_1$. A close frequency f_4 for f_1 seems to be a nonradial frequency affected by 1 cycle day^{-1} aliases.

SXP2: During the pre-whitening processes, we have detected five more frequencies whose amplitude signal-to-noise ratio is larger than 3.6. But we could only confirm three frequencies with their amplitude signal-to-noise ratios larger than 4.0 (see Table 3). The former two frequencies, f_1 and f_2 seem to be a pair of double-radial mode, and the latter f_3 is a combination frequency corresponding to $f_1 + f_2$. Probably f_3 was affected by 1 cycle day^{-1} aliases. The superimposed synthetic light curves of SXP2 in Figure 3 are calculated using f_1 and f_2 only. In Figure 4, some frequency peaks are shown in the lower panel of SXP2. To confirm these frequencies, better data are needed.

SXP3: During the pre-whitening processes we have detected six frequencies whose amplitude signal-to-noise ratios are larger than 3.7. But we can only confirm three frequencies: $f_1 = 25.8994$, $f_2 = 25.4323$ and $f_3 = 32.7041 \text{ cycles day}^{-1}$. Two frequencies, f_1 and f_3 , might be a pair of double-radial mode, and f_2 be a nonradial mode affected by 1 cycle day^{-1} alias effect. Among the rest of six frequencies a peak of $28.1463 \text{ cycles day}^{-1}$ in Figure 4 seems to be an intrinsic one. But the amplitude signal-to-noise ratio is only 3.7. To confirm this frequency, better data are needed.

NH27: NH27 is the brightest star among the nine SX Phoenicis stars in NGC 5466. We have detected four frequencies with their amplitude signal-to-noise ratios larger than

4.0 (see Table 3). f_2 and f_3 show close frequencies to f_1 . The primary frequency f_1 has a higher priority of a radial mode frequency among three close frequencies considering the higher amplitude and the existence of a harmonic frequency. But the primary frequency f_1 is also latent nonradial mode with the other two close frequencies. Though f_2 is a lower frequency (i.e. a longer period) than that of the primary frequency f_1 , it seems to be a nonradial mode. f_3 can be explained by the excitation of a nonradial mode, too. These closely separated nonradial mode frequencies were found in several recent observations of the SX Phoenicis stars (Jeon et al. 2001, 2003). The amplitude signal-to-noise ratio of f_4 is only 4.0, but its frequency 39.4356 cycles day⁻¹ is identical with $2f_1$. In Figure 4 the fourth frequency of NH27 is shown to be distinct. It is probably a harmonic frequency of the primary frequency f_1 . We can see easily the asymmetric shape of the harmonic frequency and amplitude modulating feature by closely separated frequencies in Figure 3. The frequency ratios are $f_2/f_1 = 0.985$ and $f_1/f_3 = 0.980$.

NH29: The oscillating feature of NH29 is very abnormal. It shows a distinct long period variable feature as shown in Figure 3. The period of long-term variation is 2.3430 days (see Figure 6). f_2 of NH29 is a radial frequency with total V amplitude of 0.138 mag.

NH35: Five frequencies with the amplitude signal-to-noise ratio ≥ 5.0 are detected from multiple-frequency analysis for NH35. f_1 and f_5 are radial mode ones described in § 3.1. f_2 , f_3 and f_4 are harmonic or combination frequencies corresponding to $2f_1$, $3f_1$ and $f_5 - f_1$, respectively. The total V amplitude is 0.730 mag. This star shows a typical feature of HADS stars with only one or two stable frequencies and high amplitude (typically $\Delta V \geq 0.4$ mag) compared to the feature of complicated oscillation pattern and several frequencies with low amplitude (typically $\Delta V \leq 0.05$ mag) of low amplitude δ Scuti (LADS; Petersen & Christensen-Dalsgaard (1996)) stars.

NH38: NH38 is located near a brighter star as seen in Figure 1, so observing data

obtained with bad seeing conditions were not useful. Four frequencies are detected for NH38. The primary and third frequencies, f_1 and f_3 , show a possibility of double-radial mode pair explained § 3.1. f_2 and f_4 seem to be harmonic frequencies of f_1 corresponding to $2f_1$ and $3f_1$. In Figure 4 there are two more frequencies peaked on the left side of f_3 , but their amplitude signal-to-noise ratios are too low to confirm them.

NH39: NH39 is isolated well, so hardly affected by seeing conditions. We detect six frequencies with the amplitude signal-to-noise ratio ≥ 4.1 . f_1 and f_3 are identified radial mode frequencies by the their period ratio. f_2 , f_4 and f_6 are harmonic or combination frequencies corresponding to $2f_1$, $f_3 - f_1$ and $f_3 + f_1$, respectively. A closely separated frequency of f_1 is detected by f_5 with the amplitude signal-to-noise ratio of 5.1. NH39 also shows a characteristics of HADS stars, like NH35, with the total V amplitude, 0.460 mag.

NH49: Comparing to $\langle V \rangle$ magnitudes, period and V amplitudes of the primary periods (Nemec & Mateo 1990), this is identified as NH49. NH49 has a radial mode frequency f_1 and a harmonic frequency f_2 . This star is a mono-periodic pulsator.

REFERENCES

- Breger, M. 2000, ASP Conf. Series, vol. 210, pp.3-42
- Breger, M., Stich, J., & Garrido, R., et al. 1993, A&A, 271, 482
- Chen, J. & Corwin, T.M. 1999, IBVS, no. 4708
- Clement, C. M., Muzzin, A., Dufton, Q., Ponnanpalam, T., Wang, J., Burford, J., Richardson, A., Rosebery, T., Rowe, J., & Sawyer Hogg, H. 2001, AJ, 122, 2587
- Gilliland, R.L., & Brown, T.M. 1988, PASP, 100, 754
- Handler, G., Balona, L.A., Shobbrook, R.R., Koen, C., Bruch, A., Romero-Colmenero, E., Pamyatnykh, A.A., Willems, B., Eyer, L., James, D.J., & Maas, T. 2002, MNRAS, 333, 262
- Harris, H.C. 1996, AJ, 112, 1487 (<http://physun.physics.mcmaster.ca/Globular.html>; revised in February 2003)
- Henry, G.W., Fekel, F.C., Henry, S.M. 2004, AJ, 127, 1720
- Jeon, Y.-B., Kim, S.-L., Lee, H., & Lee, M.G. 2001, AJ, 121, 2769
- Jeon, Y.-B., Lee, M.G., Kim, S.-L., & Lee, H. 2003, AJ, 125, 3165
- Kallrath, J., Milone, E.F., & Stagg, C.R. 1992, ApJ, 389, 590
- Kim, S.-L., & Lee, S.-W. 1995, J. Korean Astron. Soc., 28, 197
- Lee, H., Jeon, Y.-B., Kim, S.-L., & Park, H. S. 2003, in preparation.
- Massey, P., & Davis, L.E. 1992, A User's Guide to Stellar CCD photometry with IRAF
- Mateo, M., Harris, H.C., Nemec, J., & Olszewski, E.W. 1990, AJ, 100, 469

- McKinley, C., & Corwin, T.M. 1998, IBVS, no. 4619
- McNamara, D.H. 1995, AJ, 109, 1751
- McNamara, D.H. 2000, PASP, 112, 1096
- McNamara, D.H. 2001, PASP, 113, 335
- Nemec, J., & Harris, H.C. 1987, ApJ, 316, 172
- Nemec, J., & Mateo, M. 1990, ASP Conf. Ser., 11, 64
- Nemec, J.M., Nemec, A.F.N., & Lutz, T.E. 1994, AJ, 108, 222
- Petersen, J.O., Christensen-Dalsgaard, J. 1996, A&A, 312, 463
- Pych, W., Kaluzny, J., Krzeminski, W., Schwarzenberg-Czerny, A., & Thompson, I.B. 2001, A&A, 367, 148
- Rodríguez, E., Costa, V., Handler, G., and García, J.M. 2003, A&A, 399, 253
- Rodríguez, E., & López-González, M.J. 2000, A&A, 359, 597
- Rodríguez, E., López-González, M.J., & López de Coca, P. 2000, A&AS, 144, 469
- Santolamazza, P., Marconi, M., Bono, G., Caputo, F., Cassisi, S., & Gilliland, R. L. 2001, ApJ, 554, 1124
- Stetson, P.B. 1987, PASP, 99, 191
- Templeton, M., Basu, S., & Demarque, P. 2002, ApJ, 576, 963

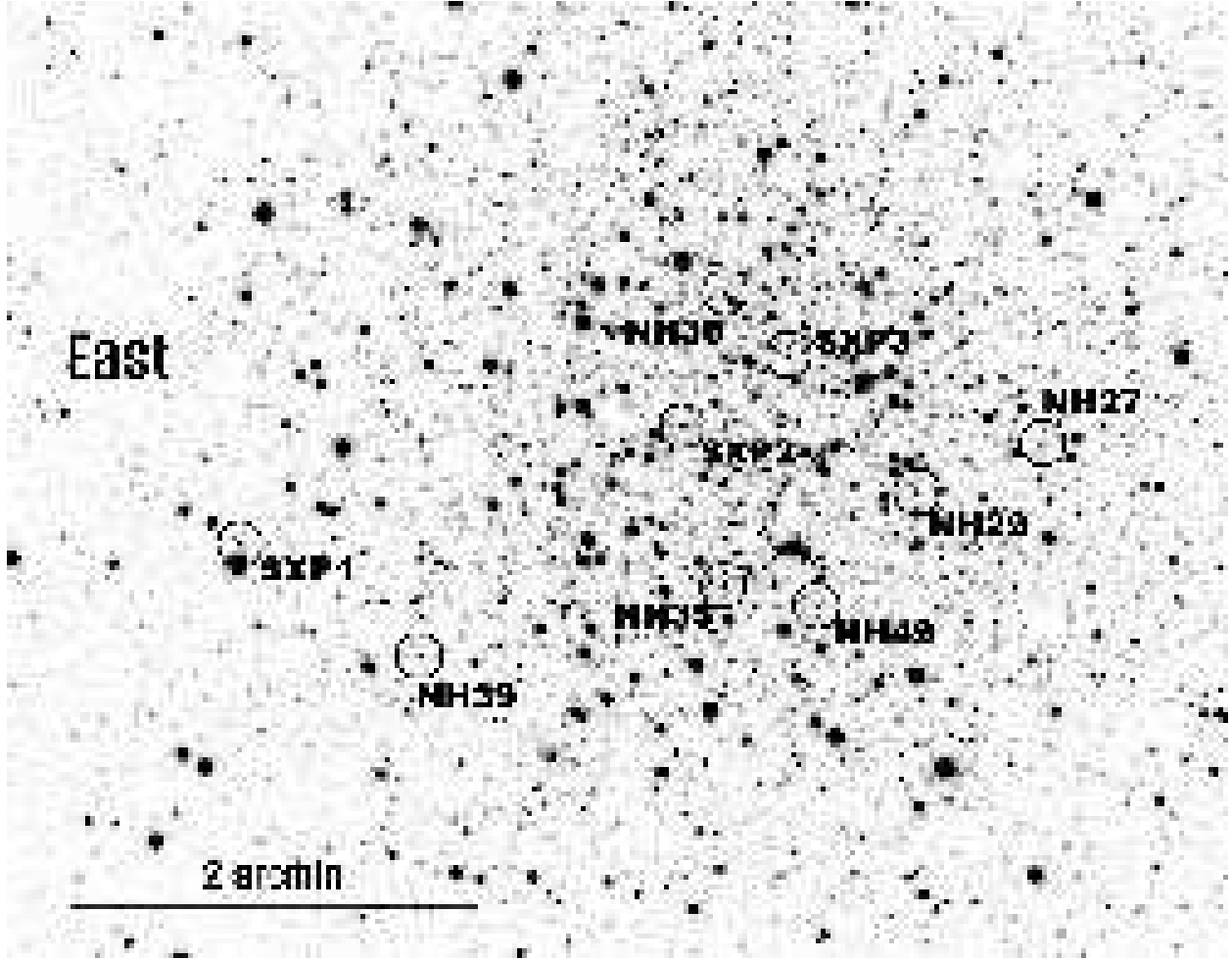


Fig. 1.— A greyscale map of a V -band CCD image of the globular cluster NGC 5466. The image is presented only for the central region ($7'.6 \times 5'.7$) of the cluster, out of the total observing field of $11'.6 \times 11'.6$. Nine SX Phoenicis stars are labeled their names.

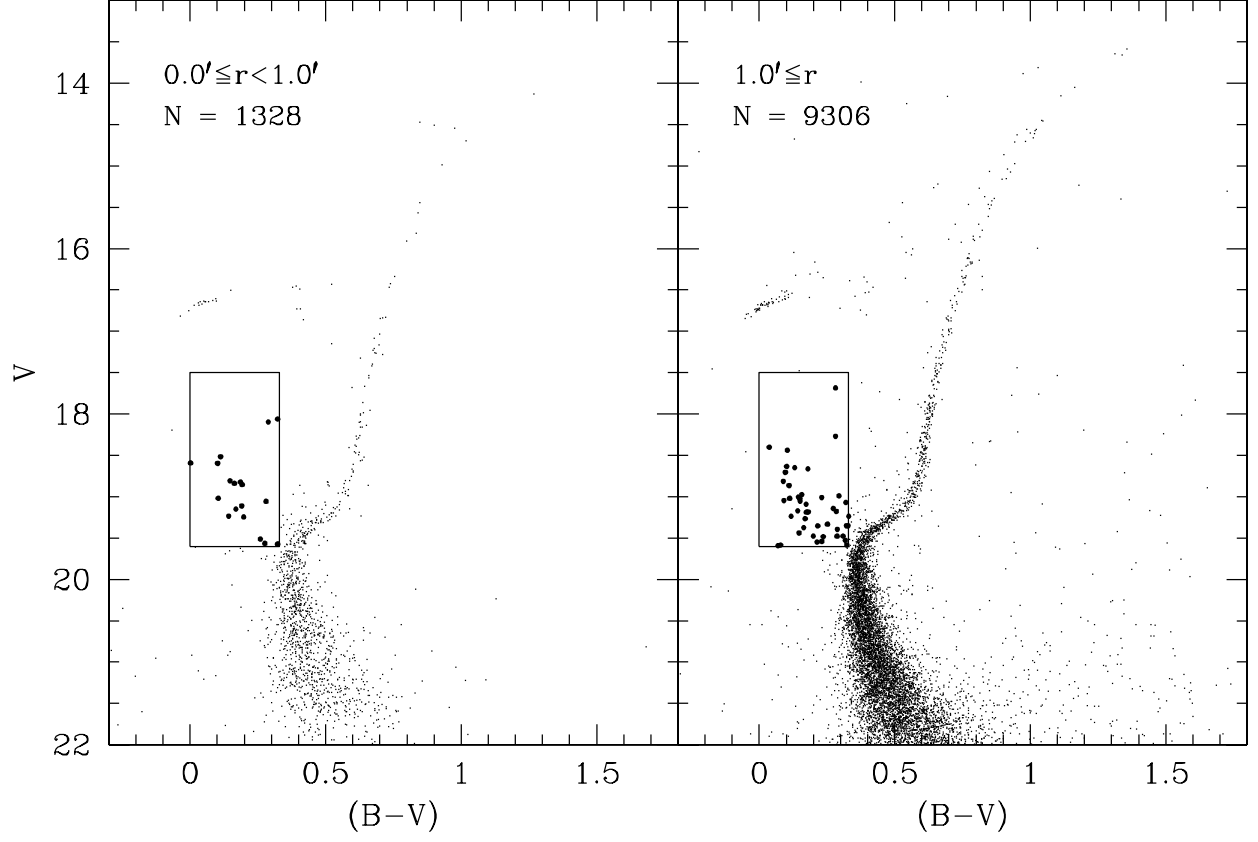
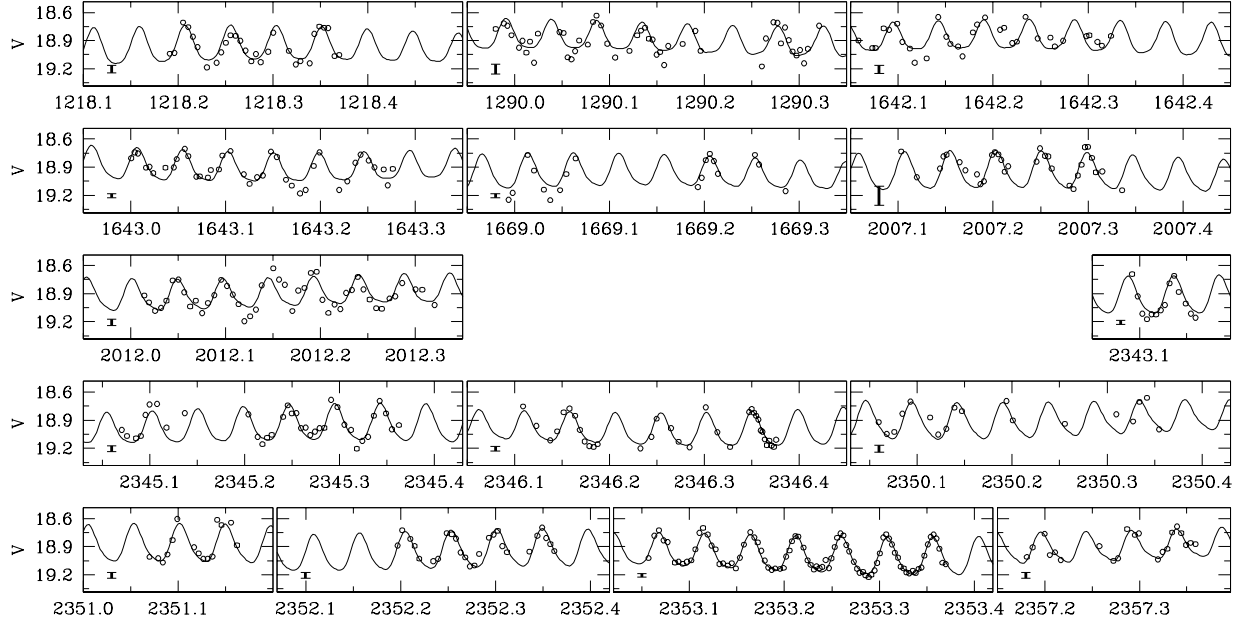


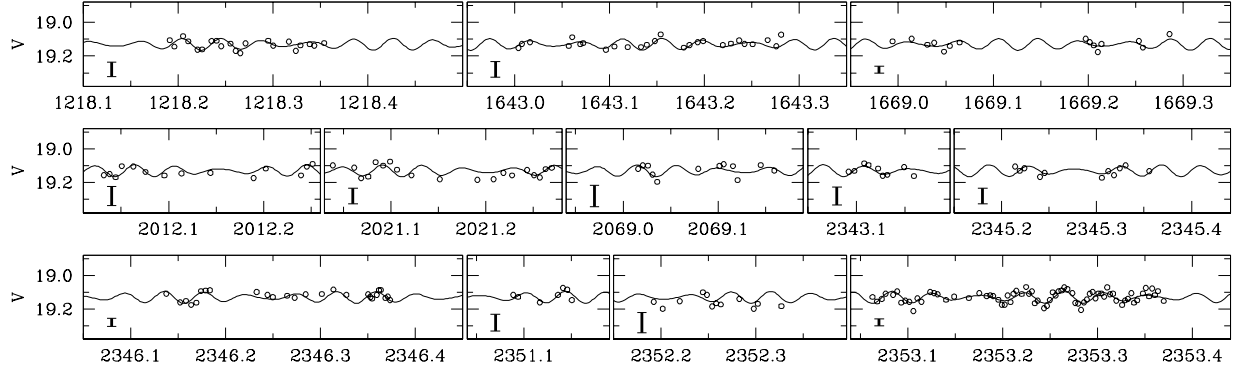
Fig. 2.— Color-magnitude diagrams of NGC5466. The left panel is for a central region at $r < 1.0'$ and the right panel is for an outer region at $r \geq 1.0'$. A blue straggler region is outlined by a box.

SXP1



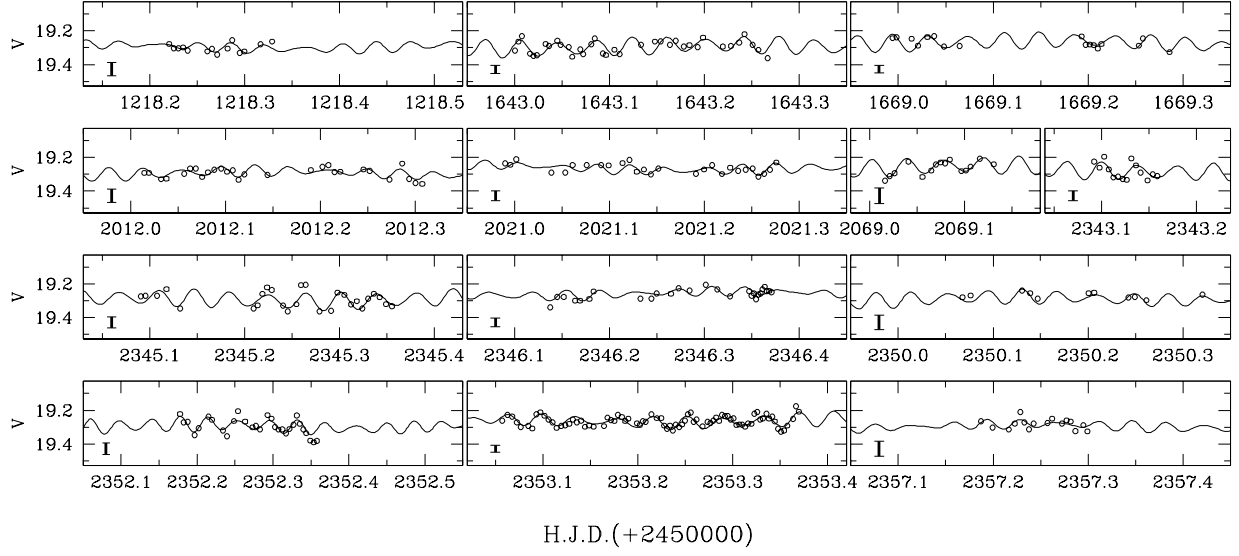
H.J.D.(+2450000)

SXP2

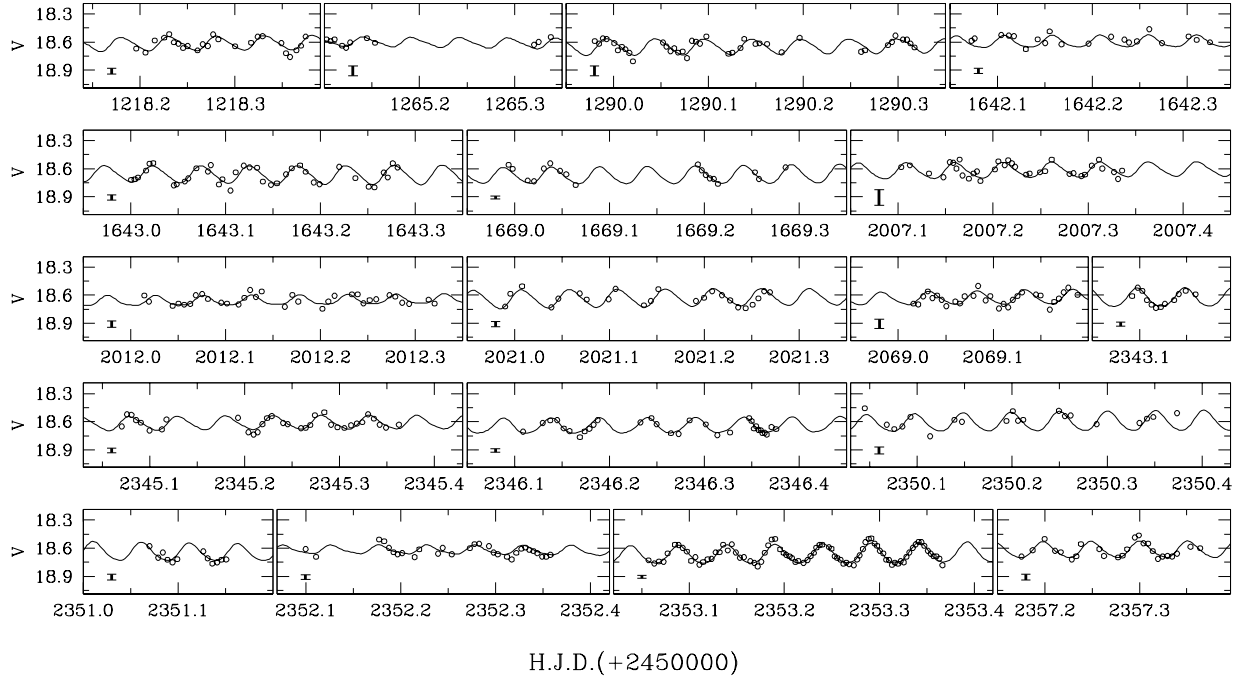


H.J.D.(+2450000)

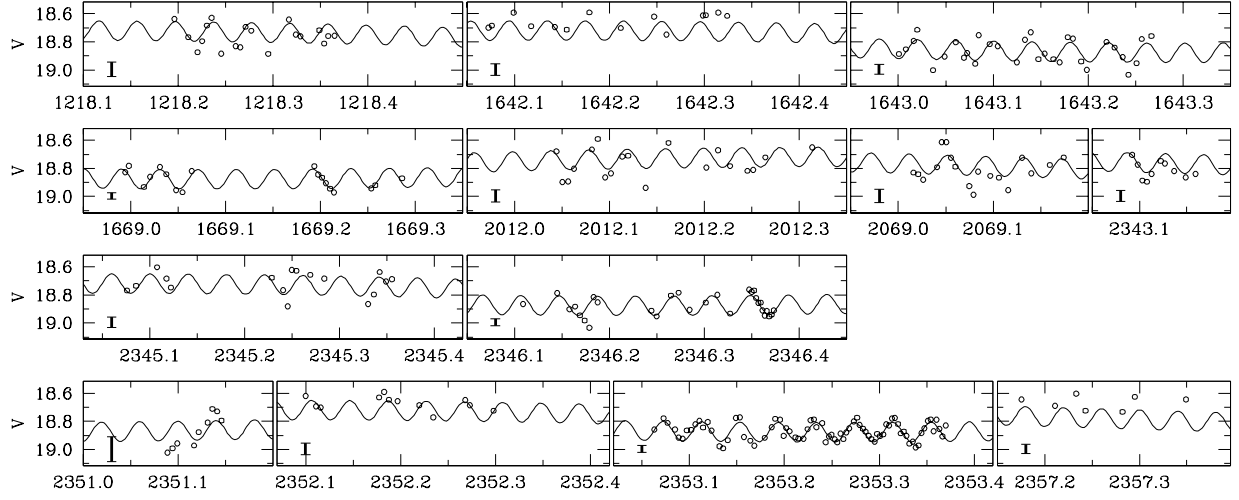
SXP3



NH27

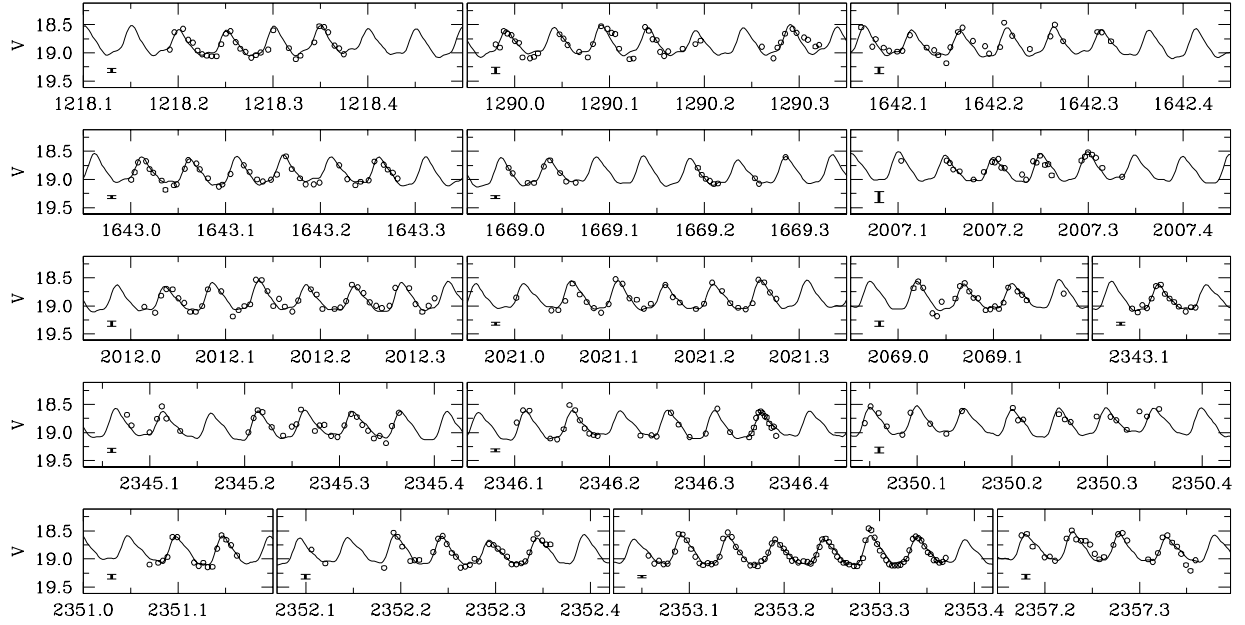


NH29

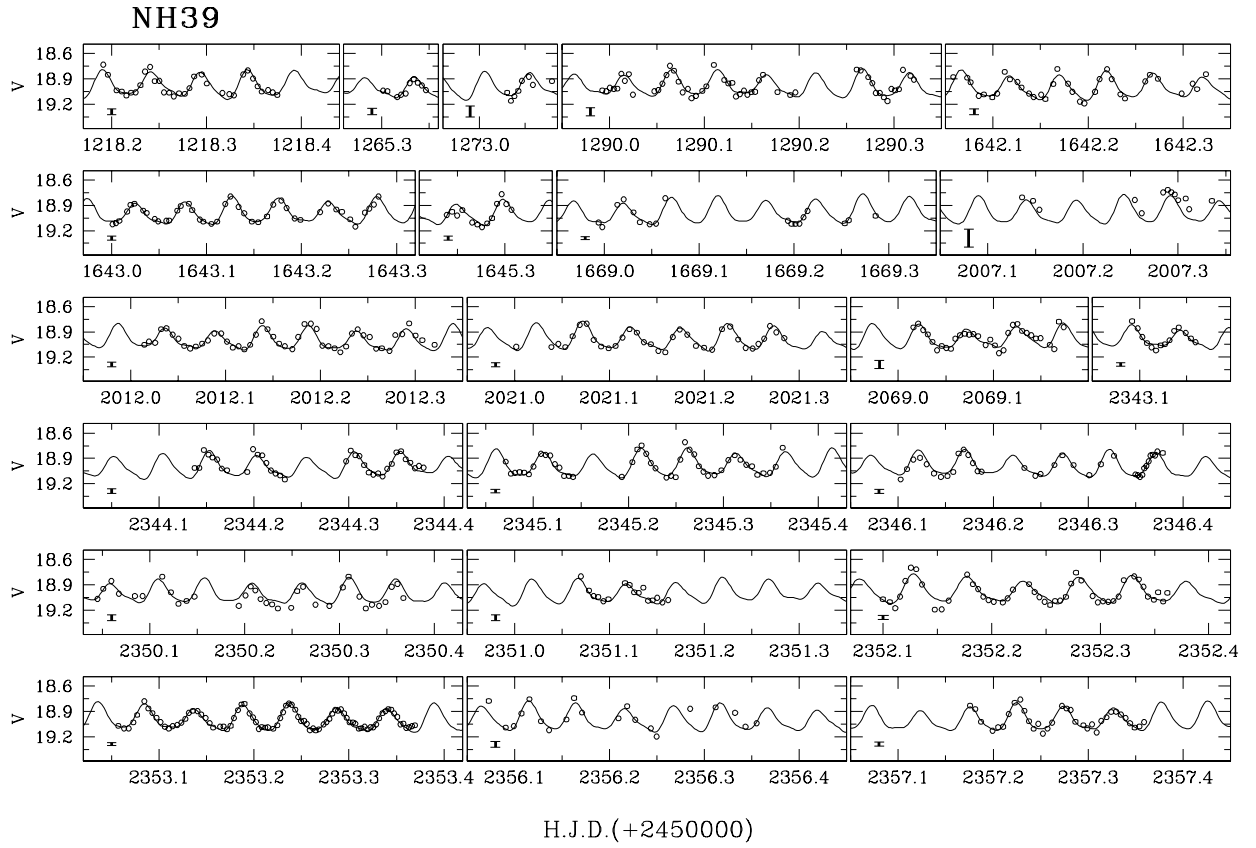
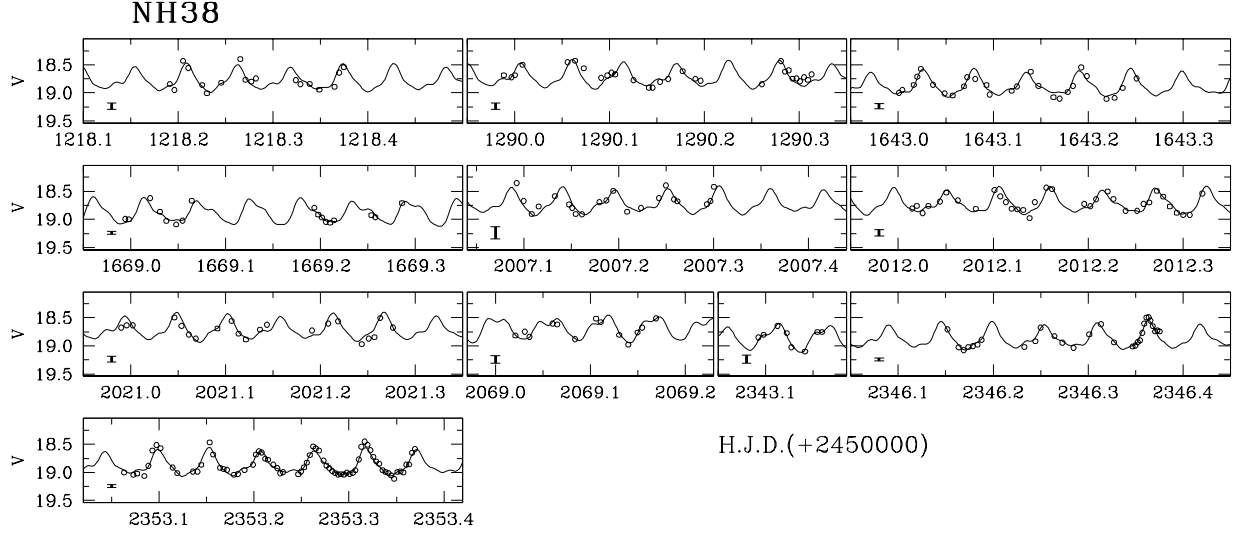


H.J.D.(+2450000)

NH35



H.J.D.(+2450000)



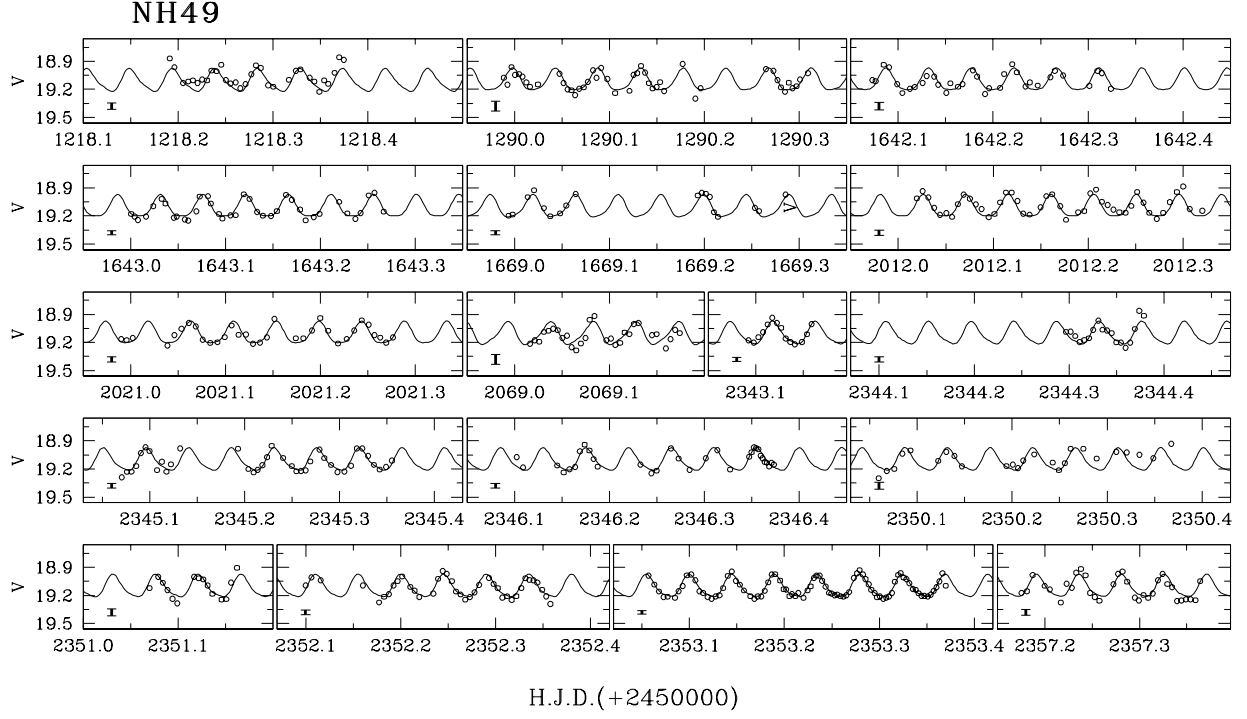
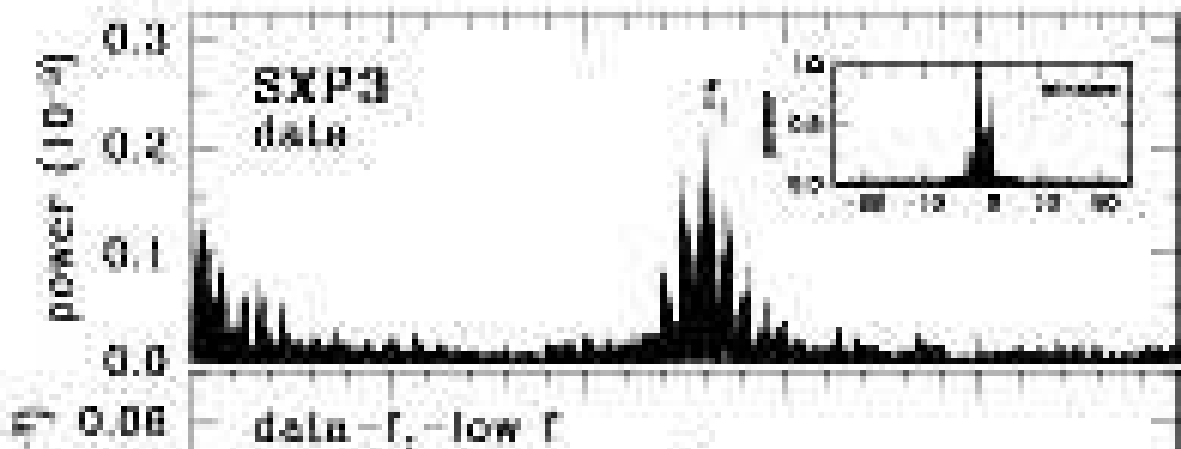
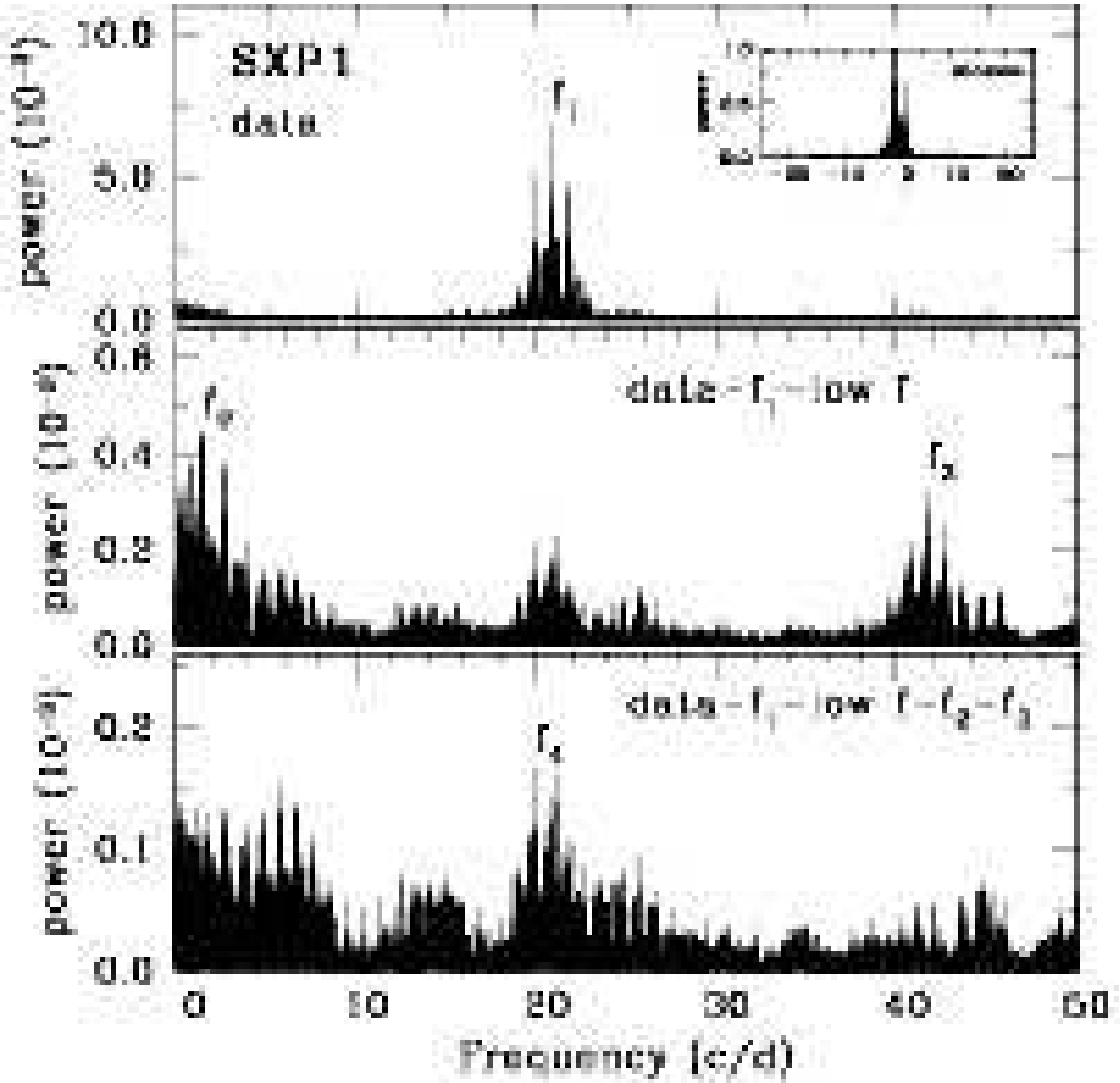
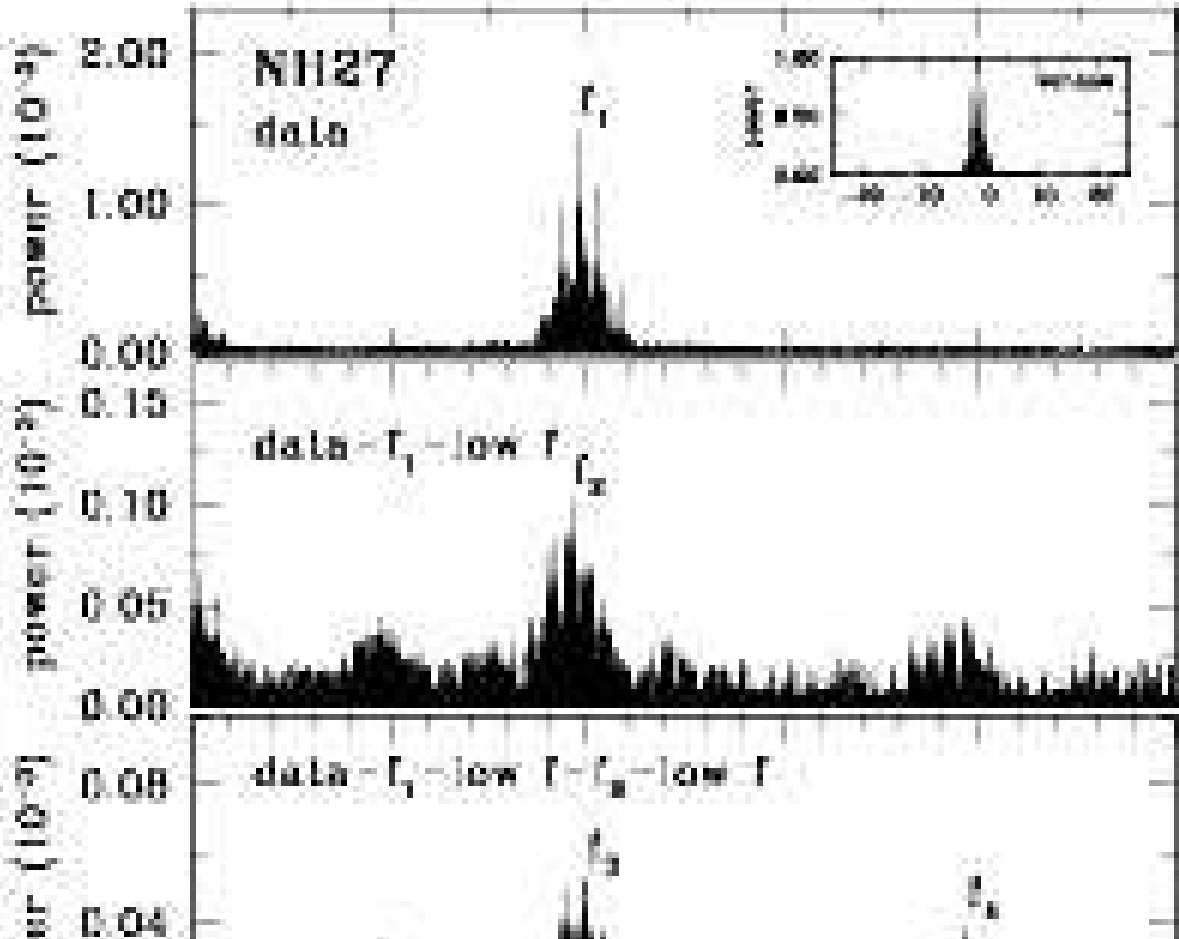
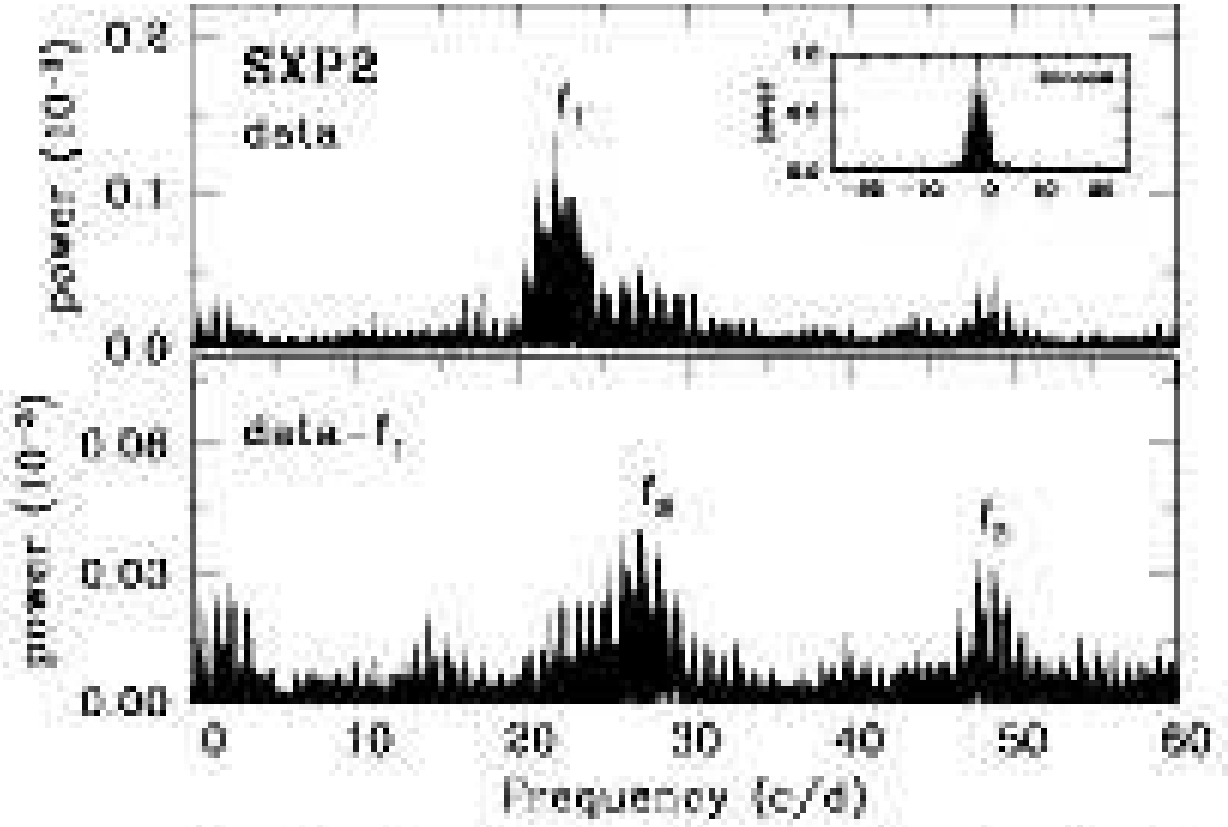
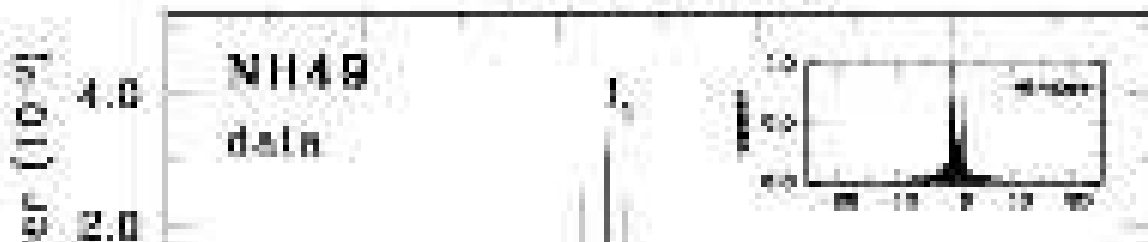
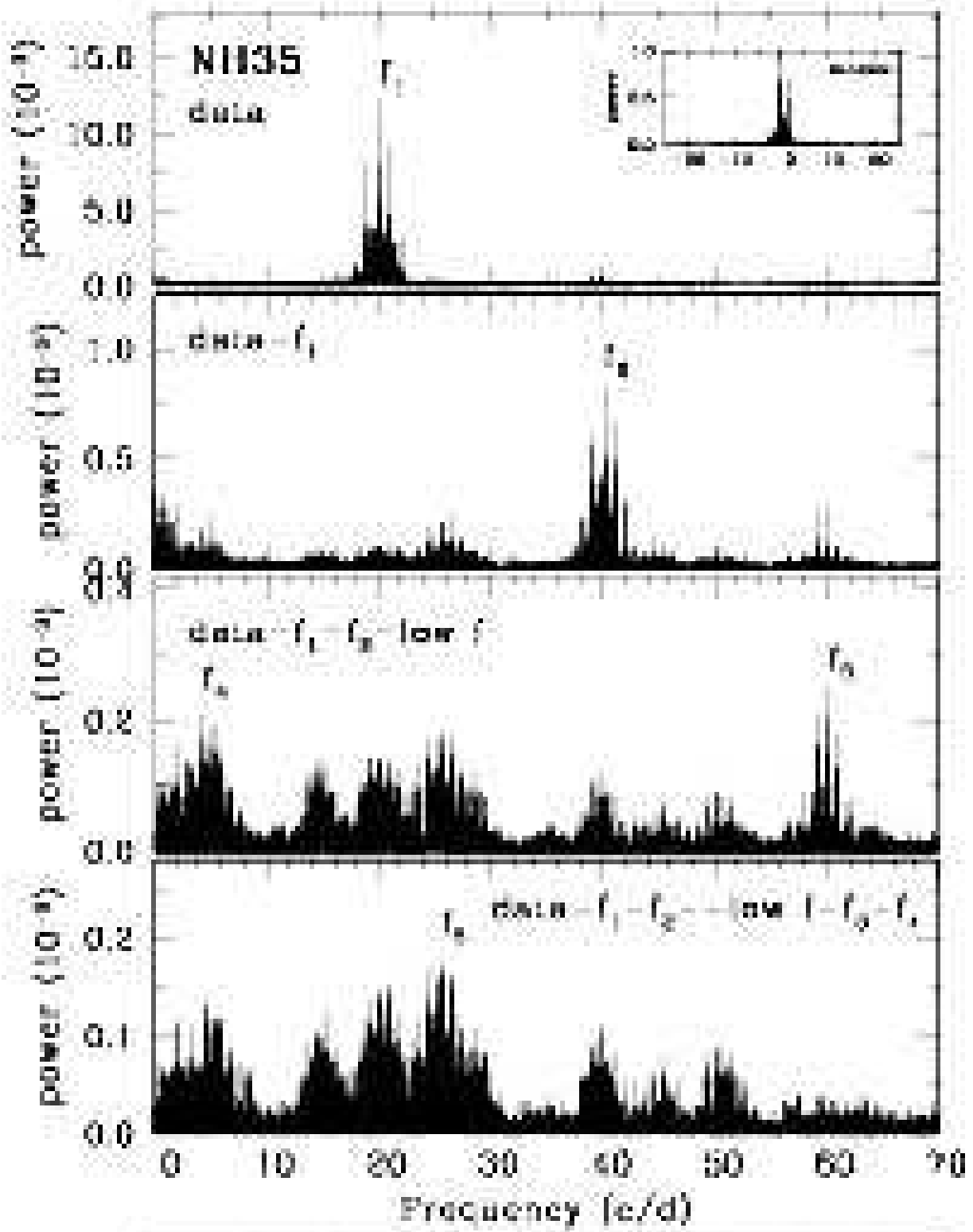


Fig. 3.— Observed data (circles) for nine SX Phoenicis stars. Synthetic light curves (solid lines) obtained from the multiple-frequency analysis (see Table 3) are superimposed on the data. We present the mean photometric errors of each observing days in the left lower corner of each panel.







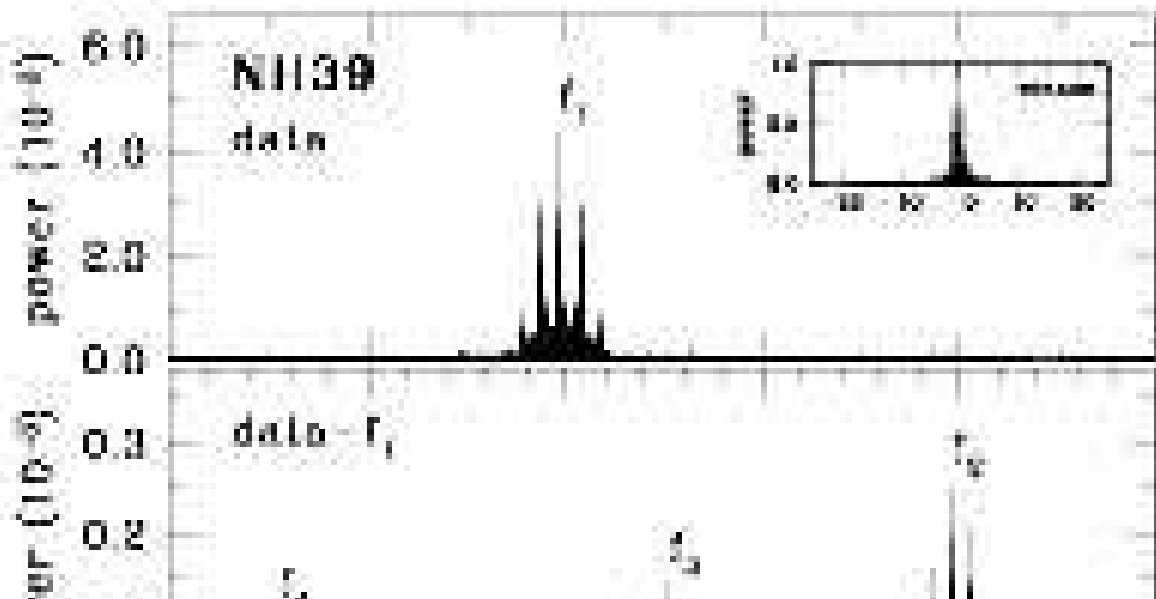
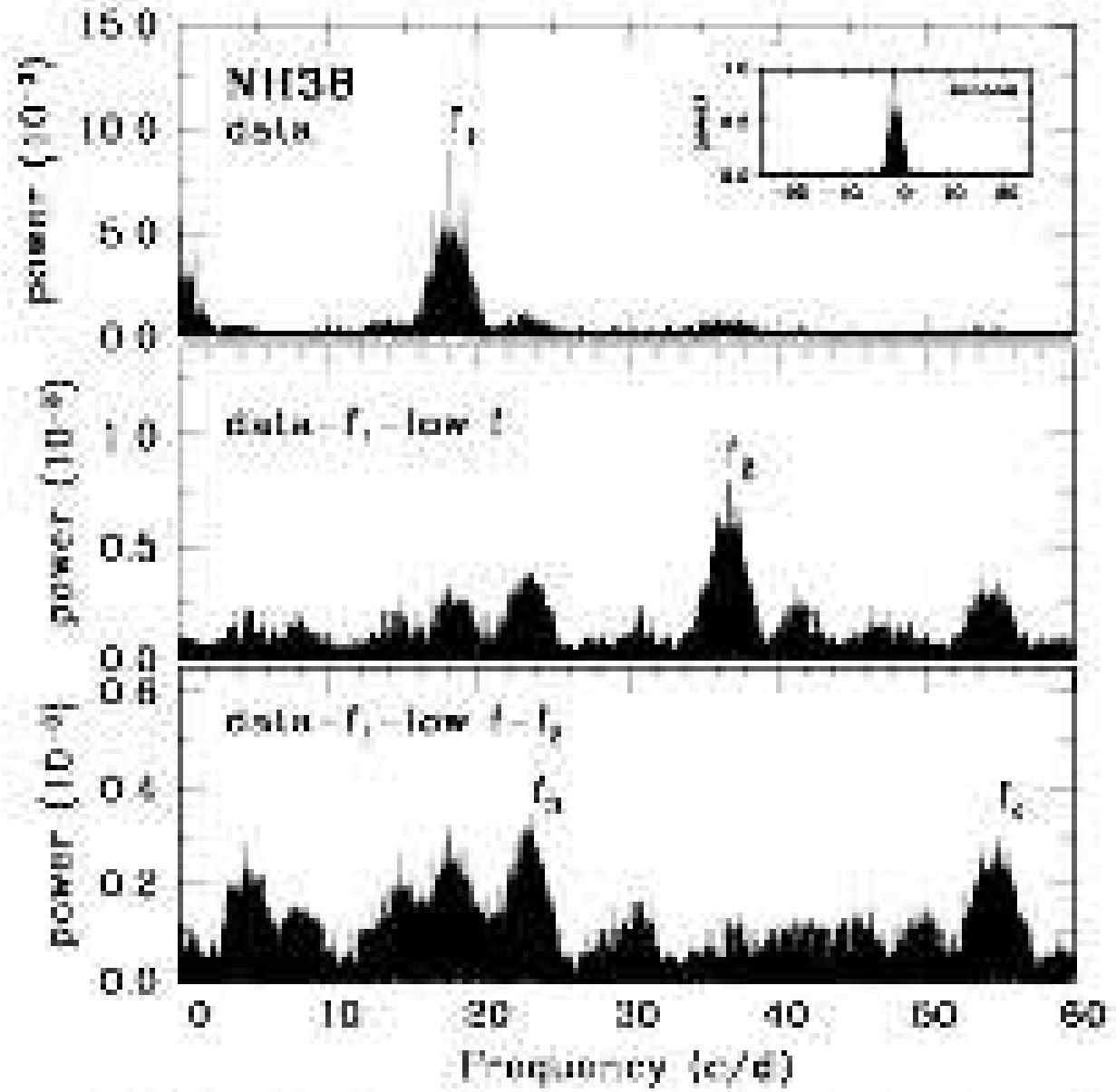


Fig. 4.— Power spectra of nine SX Phoenicis stars. Window spectra are shown in a small box within each panel.

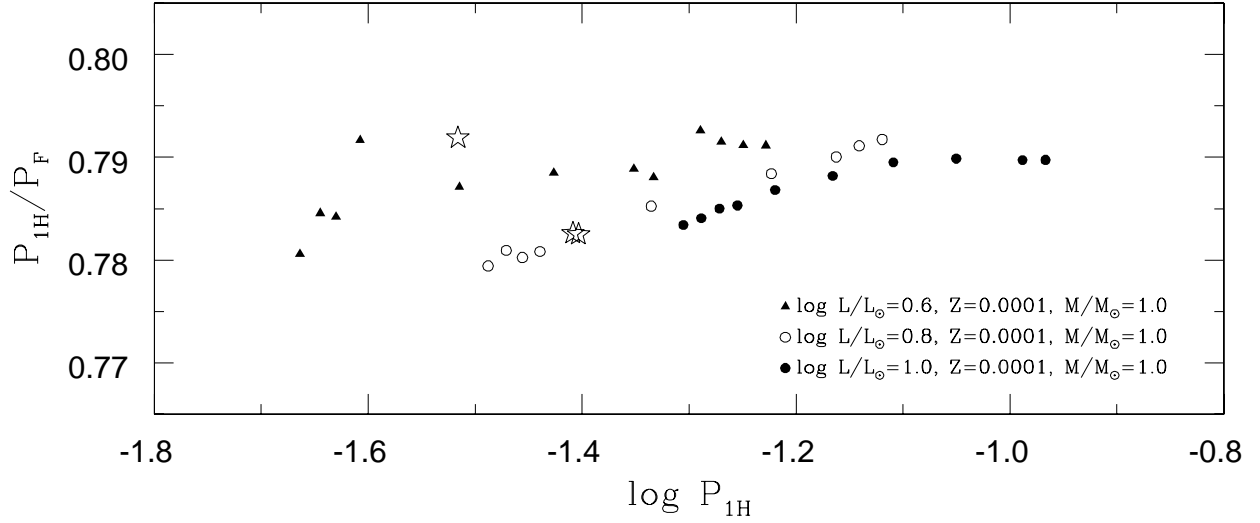


Fig. 5.— A diagram showing the period of the first overtone mode versus the period ratio of the the fundamental and first overtone modes. The theoretical period ratios of the the fundamental and first overtone modes are shown for various $\log L/L_\odot$ with $Z=0.0001$ and $M/M_\odot=1.0$ given by Santolamazza et al. (2001). Filled triangles, open circles and filled circles denote $\log L/L_\odot = 0.6, 0.8$ and 1.0 , respectively. Star symbols are the double-radial mode SX Phoenicis stars in NGC 5466.

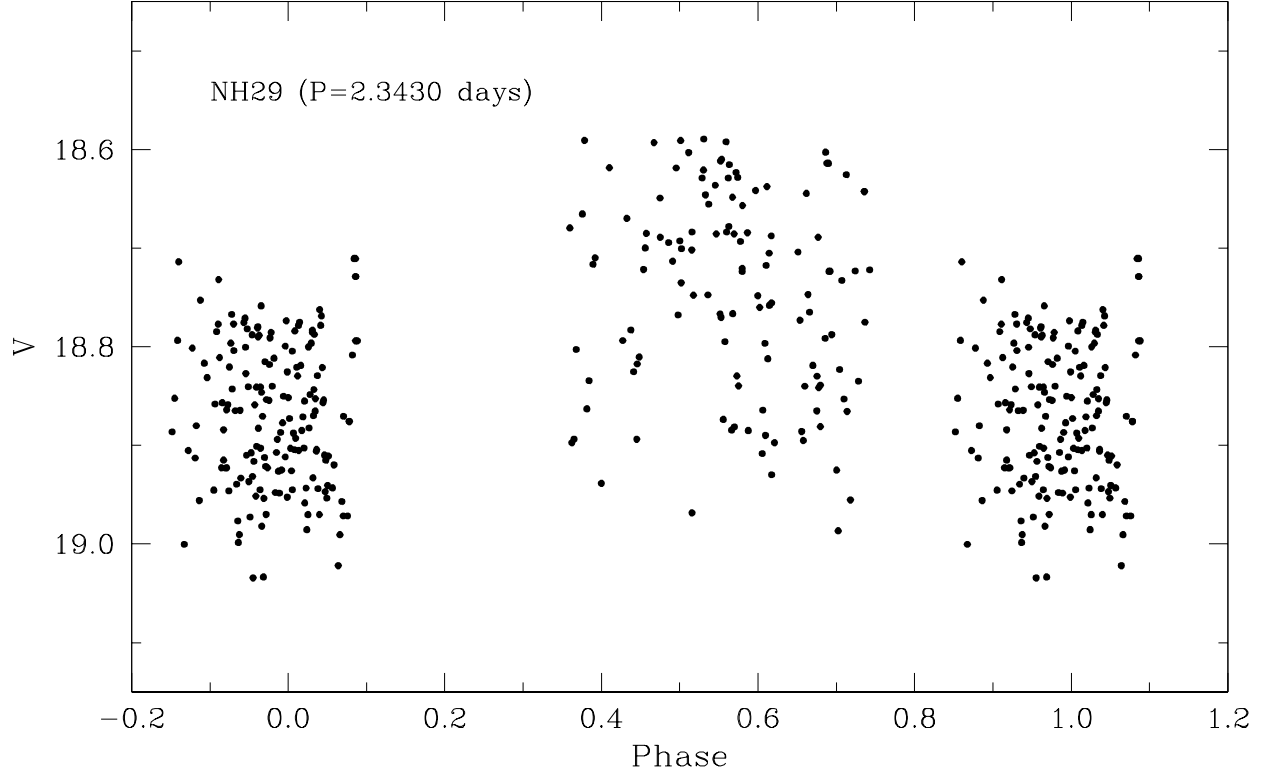


Fig. 6.— A phase diagram for the long term variations of NH29. Period and amplitude derived by multiple-frequency analyses are 2.34302 days and 0.158 mag, respectively.

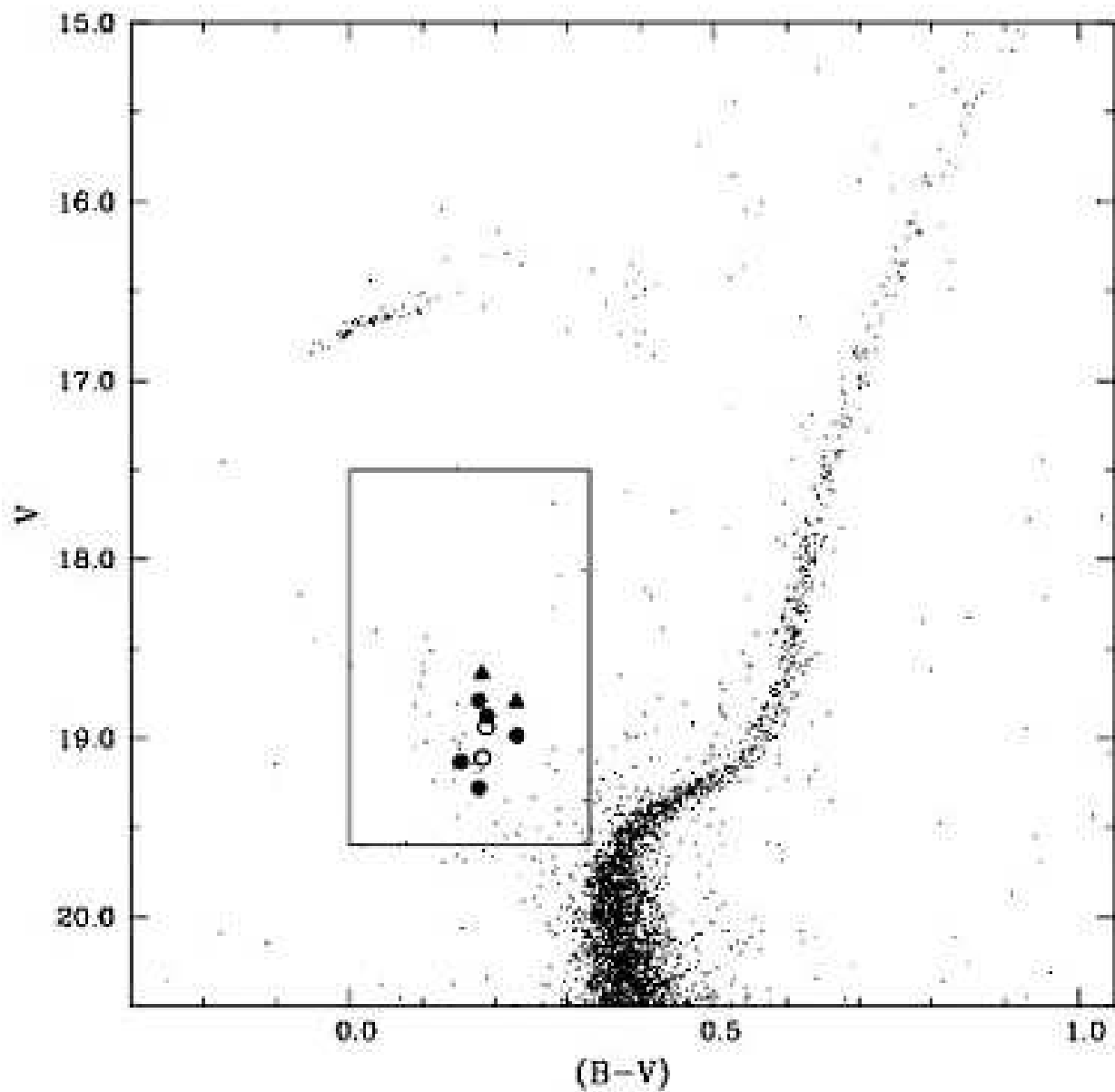


Fig. 7.— Positions of nine SX Phoenicis stars in the color-magnitude diagram of NGC 5466. Note that all they are located in the blue straggler region. A filled triangle, filled circles and open circles denote the first overtone, the double-radial mode of the fundamental and first overtone mode, and the fundamental mode pulsators, respectively.

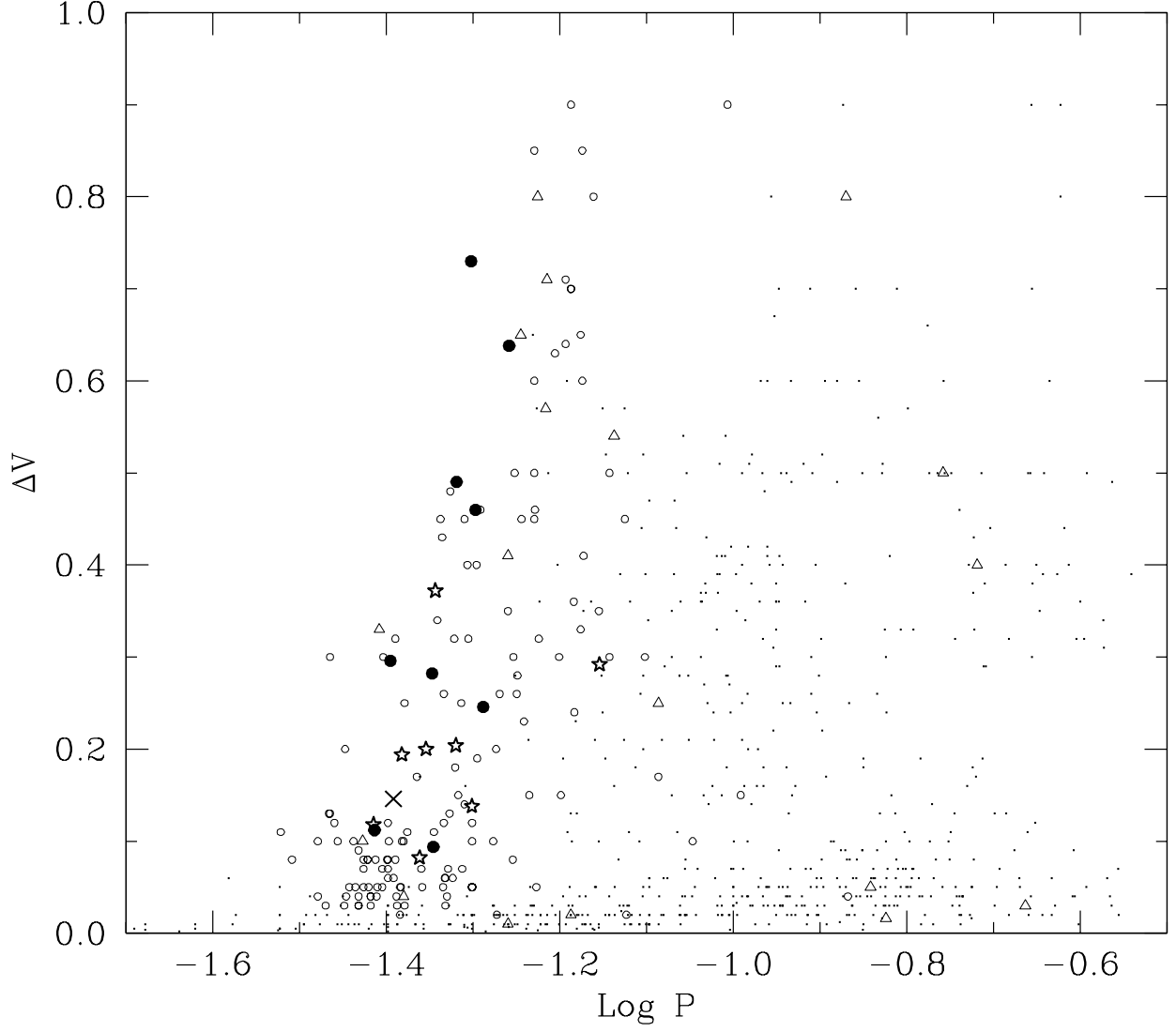


Fig. 8.— V -amplitude versus period diagram for the short period pulsating stars. Filled circles denote nine SX Phoenicis stars in NGC 5466. Star symbols and a cross denote the SX Phoenicis stars in M53 and M15, respectively, discovered in our previous search for variable blue stragglers in globular clusters (Jeon et al. 2003; Jeon et al. 2001). Triangles represent SX Phoenicis stars in the field, and open circles represent SX Phoenicis stars in other globular clusters. Dots denote δ Scuti stars.

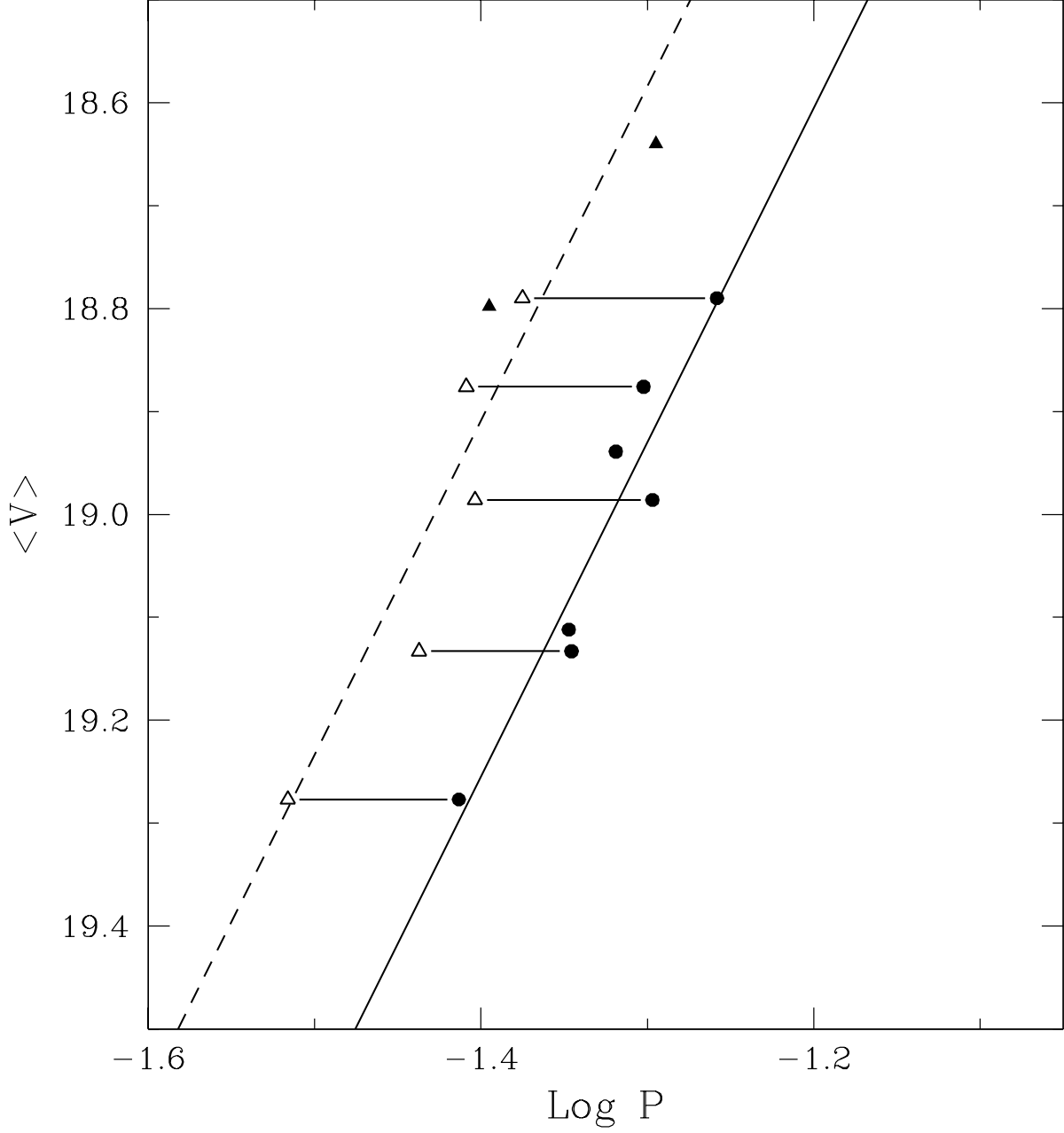


Fig. 9.— $\text{Log } P$ versus mean magnitude $\langle V \rangle$ diagram. Filled circles and filled triangles denote the fundamental and first overtone modes of SX Phoenicis stars in NGC 5466, respectively, and open triangles show the first overtone mode elements for five double-radial mode stars. A solid line represents a P-L relation for the SX Phoenicis stars with funda-

mental mode, and the line is shifted to a dashed line corresponding to a P-L relation for the first overtone mode stars by the ratio $P_{1H}/P_F = 0.783$.

Table 1. Observation Log.

Date (UT)	Start HJD (2,450,000+)	Duration (hours)	N_{obs}	Seeing (arcsec)	Exposure Time (seconds)	Remarks
1999 2 8	1218.191(<i>V</i>)	4.4	32(<i>V</i>)	1.5~1.9	300(<i>V</i>)	
1999 3 27	1265.087(<i>V</i>)	6.2	56(<i>V</i>)	2.8~3.4	300(<i>V</i>)	thin cloud, moon light
1999 4 4	1273.031(<i>V</i>)	3.0	28(<i>V</i>)	2.5~3.0	300(<i>V</i>)	moon light
1999 4 21	1289.980(<i>V</i>)	8.1	57(<i>V</i>)	1.8~2.2	300(<i>V</i>)	
2000 4 7	1642.038(<i>V</i>)	6.8	40(<i>V</i>)	2.4~3.0	180~210(<i>V</i>)	
	1642.044(<i>B</i>)		20(<i>B</i>)		360(<i>B</i>)	
2000 4 8	1643.001(<i>V</i>)	6.7	42(<i>V</i>)	1.3~1.8	180(<i>V</i>)	
	1643.012(<i>B</i>)		18(<i>B</i>)		360(<i>B</i>)	
2000 4 10	1644.994(<i>V</i>)	7.6	51(<i>V</i>)	2.5~4.4	300(<i>V</i>)	thin cloud
2000 5 4	1668.994(<i>V</i>)	7.0	18(<i>V</i>)	1.0~1.4	240(<i>V</i>)	many observing targets
	1669.004(<i>B</i>)		4(<i>B</i>)		360(<i>B</i>)	
2001 4 7	2007.058(<i>V</i>)	6.6	72(<i>V</i>)	1.0~1.4	200(<i>V</i>)	full moon
2001 4 12	2012.015(<i>V</i>)	7.3	49(<i>V</i>)	2.0~2.5	400(<i>V</i>)	moon light
2001 4 21	2020.990(<i>V</i>)	7.0	39(<i>V</i>)	2.0~2.5	400(<i>V</i>)	thin cloud
2001 6 8	2069.016(<i>V</i>)	4.9	40(<i>V</i>)	1.5~2.3	300(<i>V</i>)	thin cloud
2002 3 9	2343.092(<i>V</i>)	1.6	14(<i>V</i>)	1.8~2.2	300(<i>V</i>)	
2002 3 10	2344.067(<i>V</i>)	7.4	57(<i>V</i>)	2.5~4.5	300(<i>V</i>)	bad seeing
2002 3 11	2345.071(<i>V</i>)	7.0	51(<i>V</i>)	2.0~2.4	300~500(<i>V</i>)	
2002 3 12	2346.103(<i>V</i>)	6.6	44(<i>V</i>)	0.9~3.0	120~300(<i>V</i>)	many observing targets
	2346.239(<i>B</i>)		6(<i>B</i>)		150~700(<i>B</i>)	

Table 1—Continued

Date (UT)	Start HJD (2,450,000+)	Duration (hours)	N_{obs}	Seeing (arcsec)	Exposure Time (seconds)	Remarks
2002 3 16	2350.045(V)	7.8	38(V)	2.5~3.0	300~600(V)	many observing targets
2002 3 17	2351.071(V)	2.1	16(V)	2.0~2.3	300(V)	
2002 3 18	2352.100(V)	6.2	48(V)	1.8~3.2	250~400(V)	
2002 3 19	2353.057(V)	7.5	86(V)	1.0~1.3	150~300(V)	the best images
2002 3 22	2356.048(V)	7.3	30(V)	3.0~3.2	600(V)	thin cloud
2002 3 23	2357.176(V)	4.6	36(V)	2.3~3.0	300~400(V)	

Table 2. Observational Parameters of the nine SX Phoenicis Stars.

Name	R.A.(J2000.0)	Decl.(J2000.0)	$\langle V \rangle$	$\langle B \rangle - \langle V \rangle$
CI* NGC 5466 SXP 1 (New)	14 5 39.25	28 31 18.5	18.939	0.188
CI* NGC 5466 SXP 2 (New)	14 5 29.05	28 31 56.7	19.133	0.153
CI* NGC 5466 SXP 3 (New)	14 5 28.12	28 34 49.1	19.277	0.178
CI* NGC 5466 NH 27	14 5 20.72	28 31 53.4	18.640	0.182
CI* NGC 5466 NH 29	14 5 23.61	28 31 37.9	18.798	0.229
CI* NGC 5466 NH 35	14 5 28.05	28 31 8.0	18.876	0.189
CI* NGC 5466 NH 38	14 5 28.10	28 32 37.7	18.790	0.178
CI* NGC 5466 NH 39	14 5 35.06	28 30 45.2	18.986	0.230
CI* NGC 5466 NH 49	14 5 25.86	28 31 2.7	19.112	0.183

Table 3. Pulsating Properties of the Nine SX Phoenicis Stars.

Name	Value	Frequency ^{a,b}	Amp. ^b	Phase ^b	S/N ^c	Modes ^d	Remarks
Cl* NGC 5466 SXP 1	f_1	20.8404	0.171	3.6823	34.0	F	
	f_2	1.5616	0.038	0.2057	8.7	g ?	γ Dor ?
	f_3	41.6809	0.036	3.3180	7.5	$2f_1$	
	f_4	19.9596	0.026	2.8318	5.3	Nonradial ^d	
Cl* NGC 5466 SXP 2	f_1	22.1600	0.023	0.9756	9.0	F	$f_1/f_2 = 0.810$
	f_2	27.3563	0.012	-0.7726	4.9	1H ^e ?	
	f_3	47.9119	0.012	-1.5546	4.3	$f_1 + f_2$?	$f_1 + f_2 = 49.5$
Cl* NGC 5466 SXP 3	f_1	25.8994	0.031	3.6580	11.7	F	$f_1/f_3 = 0.7919$
	f_2	25.4323	0.013	0.5014	5.5	Nonradial	
	f_3	32.7041	0.012	3.6235	4.6	1H	
Cl* NGC 5466 NH 27	f_1	19.7179	0.076	3.1794	24.7	1H or Nonradial	$f_1/f_3 = 0.980$
	f_2	19.4181	0.020	1.1587	6.5	Nonradial	
	f_3	20.1126	0.015	4.3056	4.7	Nonradial	
	f_4	39.4356	0.012	0.3457	4.0	$2f_2$	
Cl* NGC 5466 NH 29	f_1	0.4268	0.079	3.9715	18.2	Eclipse ?	
	f_2	24.8362	0.069	0.7290	11.3	1H	
Cl* NGC 5466 NH 35	f_1	20.0583	0.221	2.7076	41.1	F	$f_1/f_5 = 0.7826$
	f_2	40.1167	0.056	1.6236	10.7	$2f_1$	
	f_3	60.1750	0.032	2.3160	5.9	$3f_1$	
	f_4	4.3640	0.029	3.8185	5.4	$f_5 - f_1$	
	f_5	25.6302	0.027	0.8393	5.0	1H	

Table 3—Continued

Name	Value	Frequency ^{a,b}	Amp. ^b	Phase ^b	S/N ^c	Modes ^d	Remarks
Cl* NGC 5466 NH 38	f_1	18.1207	0.189	4.4947	25.9	F	$f_1/f_3 = 0.764$
	f_2	36.6623	0.055	−0.3926	7.7	$2f_1$	
	f_3	23.7158	0.037	4.0499	5.1	1H ^e ?	
	f_4	54.7930	0.038	1.5403	4.7	$3f_1$	
Cl* NGC 5466 NH 39	f_1	19.8124	0.128	1.1796	46.6	F	$f_1/f_3 = 0.7825$
	f_2	39.6248	0.032	−0.2177	11.2	$2f_1$	
	f_3	25.3187	0.024	4.1147	8.2	1H	
	f_4	5.5092	0.019	0.4269	7.0	$f_3 - f_1$	
	f_5	19.0786	0.015	0.6885	5.1	Nonradial	$f_5/f_1 = 0.963$
	f_6	45.1339	0.012	−1.1017	4.1	$f_1 + f_3$	
Cl* NGC 5466 NH 49	f_1	22.2415	0.115	0.1169	37.6	F	
	f_2	44.4803	0.026	−0.1681	8.5	$2f_1$	

^aIn cycles per day.

^b $V = Const + \Sigma_j A_j \cos\{2\pi f_j(t - t_0) + \phi_j\}$, $t_0 = \text{HJD } 2,450,000.00$.

^cS/N = {(power for each frequency) / (average power from 0 \sim 70 cycle day^{−1} after prewhit

^dF & 1H : fundamental and first overtone radial mode, respectively; g : gravitational nonradial mode; $2f_1$, $3f_1$ & $f_3 - f_1$, etc. : combination frequencies

^eProbably affected by 1 cycle day^{-1} alias.